Universitatea „Dunărea de Jos” din Galaţi

Școala doctorală de Inginerie

PH.D. THESIS

-SUMMARY-

STRESS STATES THAT APEAR IN SHIP UNCONVENTIONAL DOUBLE HULL STRUCTURES

Author,

Adrian PRESURĂ

Scientific adivsor,

Prof. univ. dr. ing. Ionel CHIRICĂ

Seria I6 Inginerie mecanică Nr. 38

GALAŢI

2017

Universitatea „Dunărea de Jos” din Galaţi

Școala doctorală de Inginerie

PH.D. THESIS

-SUMMARY-

STRESS STATES THAT APEAR IN SHIP UNCONVENTIONAL DOUBLE HULL STRUCTURES

Author,

Adrian PRESURĂ

Scientific advisor, Prof. univ.dr.ing. Ionel CHIRICĂ

Scientific referents Prof. univ.dr.ing. Leonard DOMNIŞORU
Conf. univ.dr.ing. Ionel GAVRILESCU
Conf. univ.dr.ing. Elena-Felicia BEZNEA

Seria I6 Inginerie mecanică Nr. 38

GALAŢI

2017

SUMMARY

KEY WORDS

CAP.1 – double hull, oil tankers, bulk carriers, LNG, LPG, nuclear ships, portcontainers, submarines, technical ships, unconventional double hull, sandwich structure, impact strength, side collision, grounding.

CAP.2 – MARPOL, SOLAS, MSC.235(82), IBC Code, IGC Code, ADN, NMA 123/994.

CAP.3 – theory of elasticity, theory of plasticity, failure criterion, steel hardening, fracture mechanincs, critical energy, stress states, classification societies, finit element method.

CAP.4 – numerical simulation, meshing, boundary conidtions, local loads, global loads, material idealization.

CAP.5 – elasto-plastic deformation, experimental stand, material mechanical characteristic, thin test piece, tensile testing, bilinear charcteristic, internal energy, mesh tests.

CAP.6 – conventional double hull, inland navigation ship, longitudinal bending, quasi-static load, contact force, dynamic load, dynamic friction, structure failure, deformation energy, global deformation, local deformations.

CAP.7 – penetration distance, structure weight, feasibility, usual materials, deformable girder, polystyrene, intermediate transverse frames, ductile, arc.

CAP.8 – modernization, benefits, disadvantages.

CAP.10 – safety level, environmental pollution, direct analyze.

CAP.11 – competitive design.

CHAPTER 1
THE ACTUAL STAGE OF RESEARCH IN THE FIED

1.1 Necessity of double hull

In time because of the new rules, but also because of the new functional requirements, the double hull structures have gained a wide use in ship construtions, being designed to meet the technical requirements specific to every type of ship.

In principal, the double hull functions can be classfied in two categories:

a) general functions
- utilization of double bottom and double side spaces as tanks for ballast, fresh water, fuel oil etc.
- ensuring a minimum level of flotation and stability in case of bottom and/or side damages

b) ship type specific funtions
- oil tankers to ensure a certain level of protection of cargo tanks in case of an collision (grounding or collision with another ship), thus following the reducing the risk of spillage of oil products
- chemical products tankers, ADN tankers and FPSO: for protection of cargo tanks
- nuclear propulsion ships: protection of nuclear reactor in case of a collision
- portcontainers: to increase the torsion strength and rigidity which is affected by the large openings of the cargo holds hatches
- submarines: necessity of an internal shell resistant to pressure
- technical shps: ensuring the geometry of the cargo hold walls.

1.2 Conventional double hull structures

1.2.1 Oil tankers (CSR OT, 2012)

In CSR OT are presented typical structures of oil tankers with double hull (figure 1.6). They can be with two or three cargo tanks, with struts in central tanks or lateral tanks, with center line longitudinal bulkhead symmetric or asymmetric, with deck framing above or under the deck.

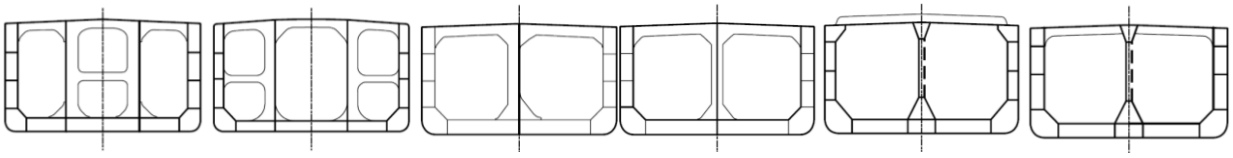

Fig.1.6 Typical sections for double hull oil tankers – (CSR OT, 2012)

1.2.2 Bulk carriers (CSR BC, 2012)

In figure 1.10 are presented the geometry of different types of bulk carriers (ABS, 2015), in order from the left:
- first section – typical Ore Carrier for transportation of ore only in central holds – two longitudinal bulkheads and double bottom
- second section – typical Oil or Bulk/Ore OBO – structure with double side and double bottom and hopper and topside tanks
- sections in the right – typical Ore or Oil Carrier for transportation of ore in central holds or oil in central/lateral holds – two longitudinal bulkheads and dounle bottom

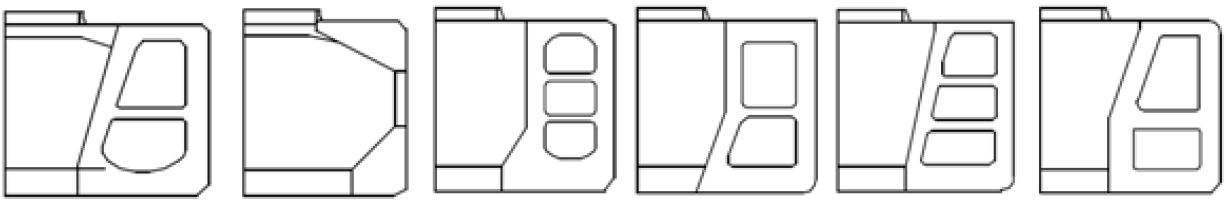

Fig.1.10 Transverse sections for different types of bulk carriers (ABS, 2015)

1.2.3 LNG, LPG (ABS, 2015)

In figure 1.11 are presented typical sections of liquid gas transportation ships, in order from the left:

- prismatic independent tank
- semi-membrane tank
- membrane tank
- spherical tank
- pressure tank

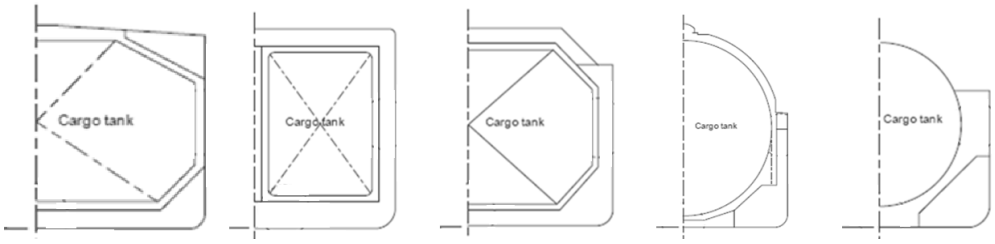

Fig.1.11 Typical structures for liquefied gas carriers (ABS, 2015)

1.2.4 ADN tanks (ADN, 2017)

Type „G" tanks for transportation of liquefied gases on inland waterways according AND can have the following configurations (figure 1.12):

- independent circular tanks with double bottom and single side
- independent circular tanks with double bottom and double side
- independent rectangular tanks with double bottom and double side

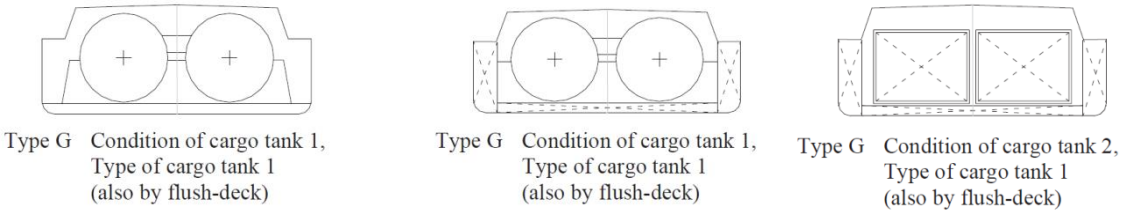

Fig.1.12 Tancuri ADN Type G – pentru transport gaze (ADN, 2017)

1.3 Unconventional double hull structures

Unconventional double hull structures appeared as a more efficient response to the requirements of collision strength, in case of a ship collision or grounding.

Below are presented a series of unconventional double hull structures which were investigated from collision strength point of view.

1.3.1 PNTL – double hull (http://www.pntl.co.uk)

PNTL (Pacific Nuclear Transport Limited) is a maritime transport company of nuclear fuel type products (MOX fuel) and the resulting waste. Considering the high risk level of this type of cargo a double side structure has been adopted which extends on 20% from the ship beam and which has an interior additional strengthened structure with horizontal 20 mm thick plates to increase the collision strentgth. The additional structure weighs approximate 400 t of steel supplementary to the ship structure, which represents approximate 40% from the mass of the steel ship conventional structure.

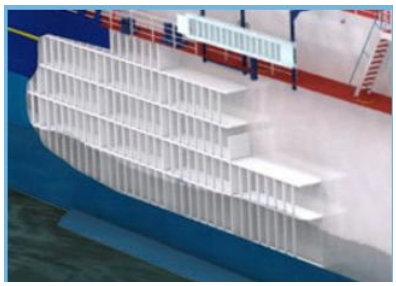

Fig.1.15 Unconventional double side – additional horizontal plates 20 mm thick (http://www.pntl.co.uk)

1.3.2 Double hull with „Y" structures (MoVe IT!, 2014)

In the European research project MoVe IT! Was analyzed a „Y" type double hull structure.

The concept is based on use of „Y" type structure elements between exterior and interior shells. In contrast with classical double hull the „Y" concept replaces the orthogonal stringers and the transverse web frames with the structure represented in figure 1.16. The „Y" shape cell as the flanges directioned to the outer shell. The geometry of the „Y" profile is described by the hight „h" of the leg, value „e" of the web, inclining angle „α" of the flanges, thickness „t" , spacing „L" and the total width „H" of the double hull structure.

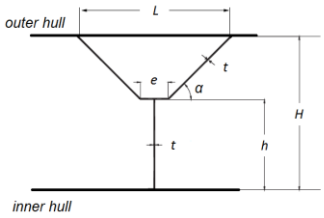

Fig.1.16 „Y" type cell structure (MoVe IT!, 2014)

1.3.3 Double hull „λ" structures (MoVe IT!, 2014)

By analogy with „Y" structures, the characteristics of „λ" structure are given fby the lateral bended plates (flanges). Un „λ" cell is described in figure 1.17.

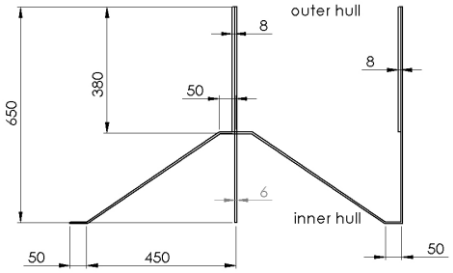

Fig.1.17 „λ" type cell structure (MoVe IT!, 2014)

1.3.4 Double hull with steel-polystirene-steel sandwich (MoVe IT!, 2014)

The concept consists of a double hull with XPS foam blocks at interior.

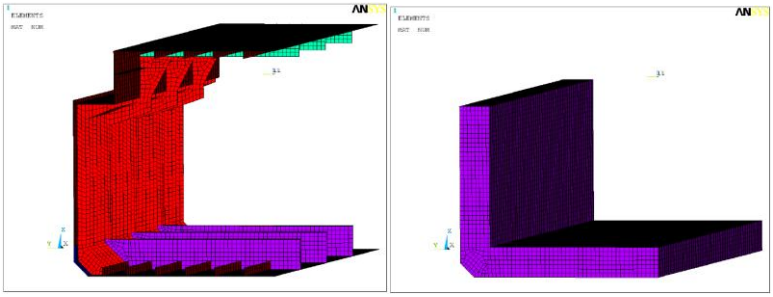

Fig.1.18 Steel elements of structure (left) foam elements of structure (right) (MoVe IT!, 2014)

1.3.5 Double hull with SPS system (http://www.ie-sps.com)

SPS is an composit material which consists of two metallic layers fixed between them with an polyurethane elastomer core. SPS is approved by the authorities in the field and is used in to a wide range of civil, maritime and special applications (military).

The SPS system is more simple and lighter than the steel panels stiffened with frames and much more lighter than reinforced concrete structures (figure 1.19), because this concept of double hull with XPS foam blocks at the interior (figure 1.20).

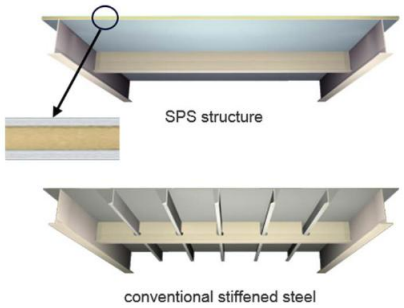

Fig.1.19 SPS panel (http://www.ie-sps.com)

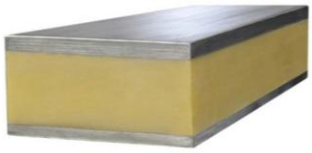

Fig.1.20 SPS element (http://www.ie-sps.com)

1.4 Actual research in the field of unconventional double hull structures

Due to increasingly stringent ship safety requirements in case of a collision and for the protection of the environment, in the case of the ships that transports dangerous goods, the idea of new unconventional double hull structures has developed to meet this requirements.

1.4.1 European research project MoVe IT! (MoVe IT!, 2014)

The FP7 MoVe IT! (2011-2014) is a European research project which has developed a series of options for economic modernization of inland navigation ships.

In the work package WP5 Structures & Weight, Task 5.3 Crashworthiness the attention was directed to selection of a typical structure for modernization and to simulation of collision strength with help of explicit dynamic method for certain accident scenarios (the impact with another ship and with the bottom of the water).

Have been investigated collision and grounding scenarios in which were varied different parameters like: the structure of hited ship („Y", „λ" or steel-foam sandwich structures), the shape of the indenter, the location and the angle of the impact.

The calculations were realized with help of ANSYS using LSDYNA explicit solver, the comparison criterion being energy absorbtion.

The model of the sigle hull structure is presented in figure 1.21.

The model of the analyzed double hull structure is presented in figure 1.22.

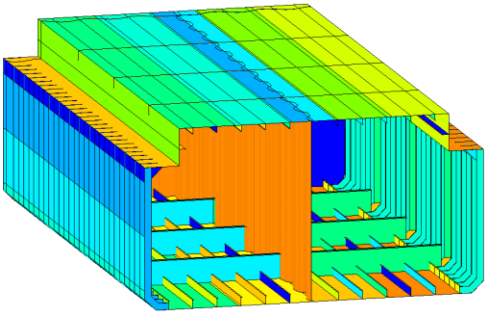

Fig.1.21 Single hull structure

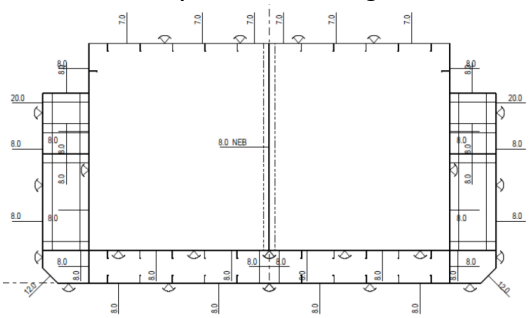

Fig.1.22 Double hull structure (MoVe IT!, 2014)

1.4.1.1 Grounding calculaions of foam structures

The typical geometries of the indenter for the bottom of the ship (figure 1.24):

- rock – dimensions much smaller than the ship, described by a parabolic curvature with 0,2 B

diameter (B ship width)

- reef – intermediate dimensions
- shoal – having the dimension of half of the ship

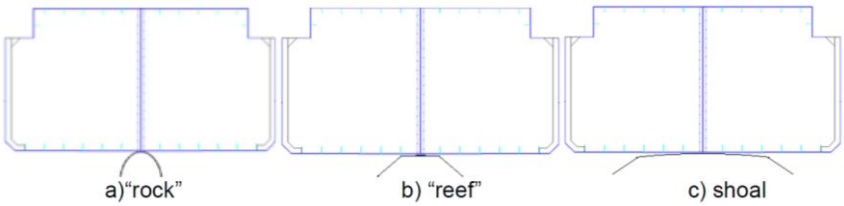

Fig.1.24 Grounding indenter geometries (MoVe IT!, 2014)

In case of the rock grounding, in location 6, the following results were obtained (figure 1.26):

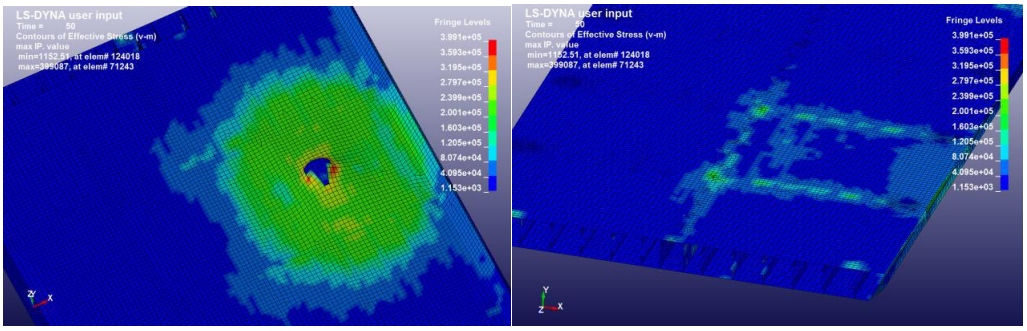

Fig.1.26 Crashing of the bottom plate and equivalent stress in inner bottom plate (MoVe IT!, 2014)

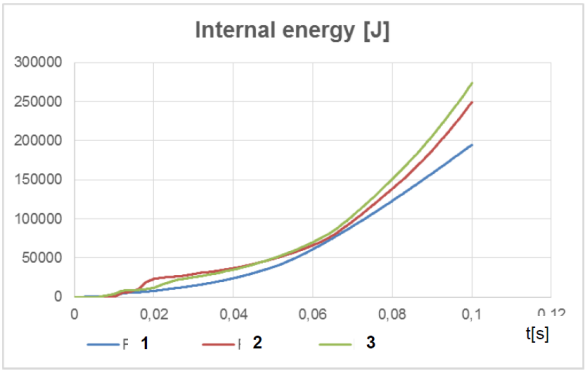

Fig.1.27 Variation of internal energy
1-single hull 2-double hull 3-double hull with foam (MoVe IT!, 2014)

The inner bottom and the foam structure absorb considerably more energy in comparison with classical double bottom structure. In figure 1.27 is shown that the internal energy of the steel-foam-steel concept is with 10% higher than internal energy of typical double bottom structure.

1.4.1.2 Lateral collision calculations of foam structures

Were considered different collision scenarios (figure 1.28):

- the speed of the striking ship varies between: 2m/s, 4m/s and 6m/s
- the relative draft between the two ships -0,5 m, 0 m and 1 m
- collision angles 90°, 60° and 45°

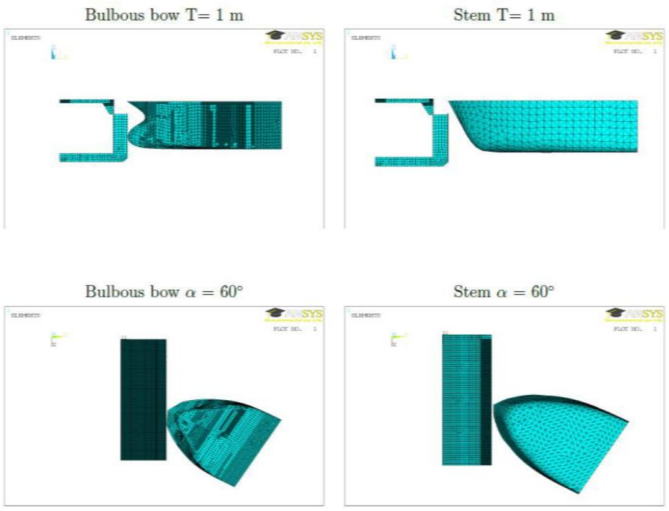

Fig.1.28 Height positioning and relative angles of the colliding bodies (MoVe IT!, 2014)

In case of a classical bow shape collision the following results were obtained (figure 1.30):

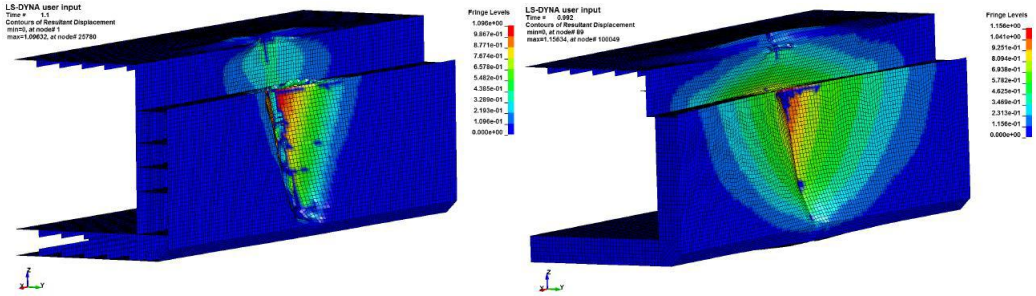

Fig.1.30 Displacements for classical double hull clasic and double hull with foam (MoVe IT!, 2014)

While classic double hull deforms rather local with appearance of a shell crack, which propagates up to the bottom of the ship, the foam structure deform more ample.

It was investigated also the influence of variation of steel and foam thickness (figure 1.31).

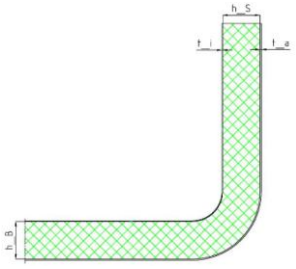

Fig.1.31 Variaţia grosimilor de oţel and de spumă (MoVe IT!, 2014)

In figure 1.32 can be observed that for the same thickness of shells, but for a double thickness of foam, respectively 400 mm (green curve) and 800 mm (yellow curve), is obtained a displacement with 0,2 m smaller.

Also by comparing the results from figures 1.32 and 1.33 it can be observed that for the same thickness of inner shell, t_i = 3 mm, and for same double side width, h_s = 400 mm, by increasing the thickness of outer sheel, t_a = 12 mm instead of 8 mm, it is obtained a reducing of displacement with 0,4 m.

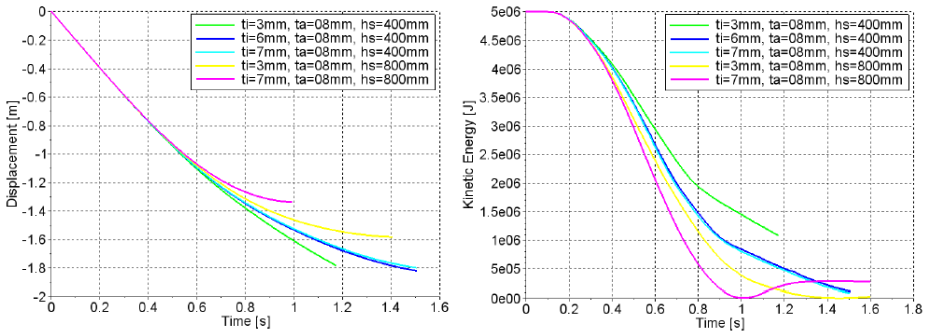

Fig.1.32 Influence of variation of steel and foam thickness for t_a=8mm (MoVe IT!, 2014)

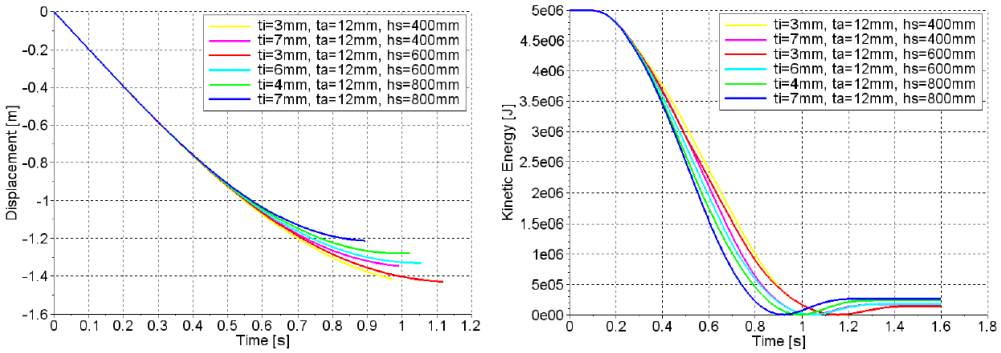

Fig.1.33 Influence of variation of steel and foam thickness for t_a=12mm (MoVe IT!, 2014)

1.4.1.3 Lateral collision calculations for „Y" and „λ" structures

In same hypotheses were analyzed also the „Y" and „λ" unconventional structures.

By comparing the figures 1.35 and 1.36 it can be observed that „Y" and "λ" double sides shows a better behavior from strength point of view in comparison with classic double hull structure because of a longer penetrating time necessary for absorbtion of the same amount of kinetic energy.

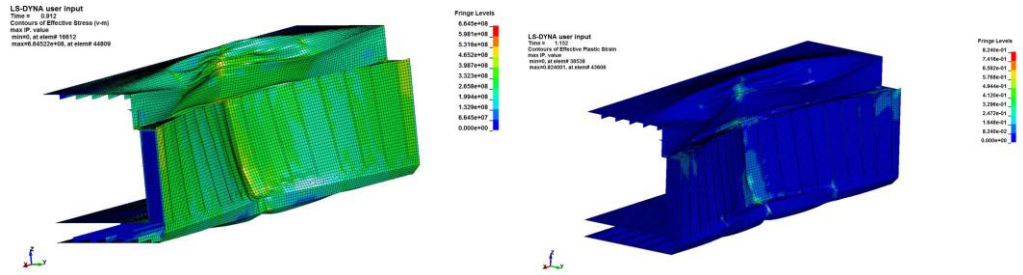

Fig.1.35 Maximum von Misses stress 577,2 MPa at 0,912s and plastic deformation at 1,152 s for „Y" double hull structure (MoVe IT!, 2014)

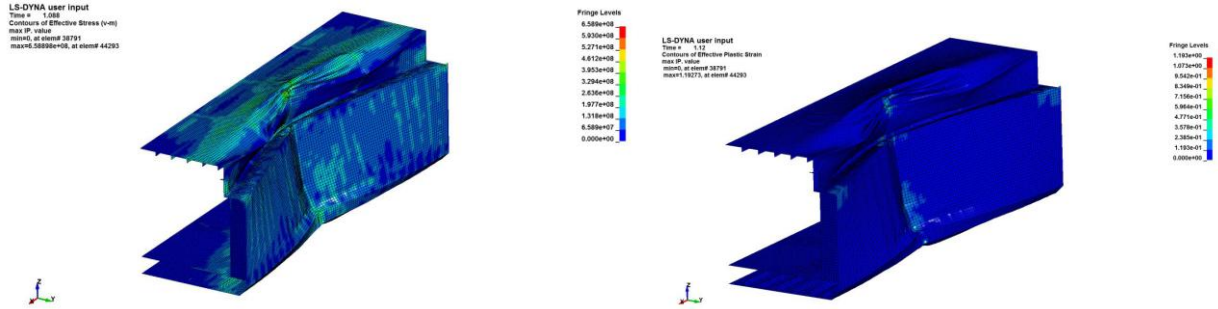

Fig.1.36 Maximum von Misses stress 658,9 MPa at 1,088s and plastic deformation at 1,12 s for „λ" double hull structure (MoVe IT!, 2014)

In figure 1.37 are presented the variations of absorbtion of internal energy and of rigid

displacement, by comparison for the three situations: classic double side, with „Y" and with „λ". The deceleration of rigid body is the biggest for the classical structure and the smallest for „Y" structure. Between the two unconventional structures „Y" and „λ" are moderate differences, but both presents a better strength than classic structure.

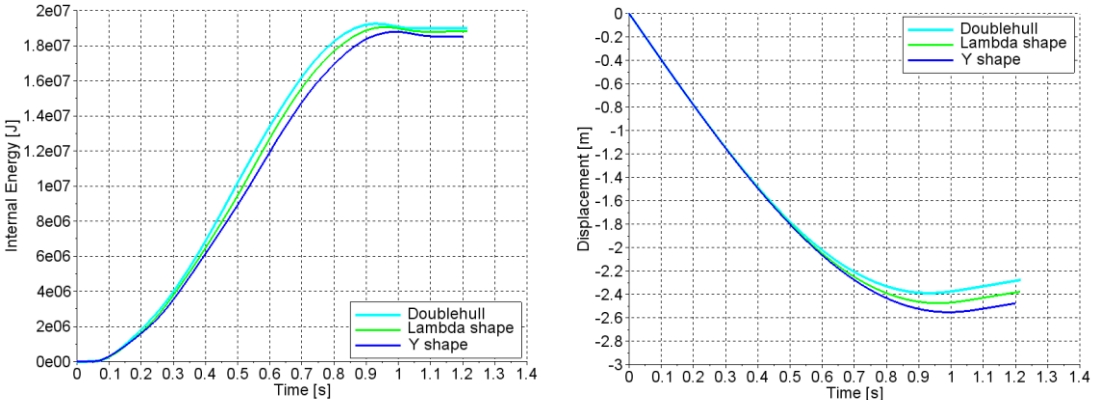

Fig.1.37 Internal energy and displacement- classic, „Y" and „λ" double side (MoVe IT!, 2014)

Conclusions of the investigations have revealed the following advantages:

- the foam from the interior can help the double hull to work like a unitary element
- sandwich type structure from steel-foam-steel has a bigger capacity for absorbtion of energy
- increased flotability in case of damage
- increasing of global strength of the double hullului.

1.4.2 SPS sandwich system (IE, 2016)

SPS system is used in military and civil applications for reducing the vulnerability and for increasing the survival and safety level. In figure 1.38 are shown the results of an explosion test done by NSWC (US Navy's Naval Surface Warfare Center) which demonstrates how the SPS panel absorbs more explosion energy, reduces the risk of premature rupture and limits the penetration of the fragments. The conventional panel of steel (left) breaks after the explosion while SPS panel (right) absorbs the energy and deforms without breaking.

Fig.1.38 Exposion testing (IE, 2016)

Fig.1.39 Rock impact testing(IE, 2016)

In figure 1.39 is presented the impact test with a 2 tones rock which is released from a 3 m distance above a deck section realized with SPS system. The SPS system resist withoud damage while the classic structure made from steel is broken.

References (IE, 2016)

The compact SPS system of double hull CDH (compact double hull) was already used in a project done in 2014, in which were involved three FPSO ships of Petrobras company (figure 1.40). The SPS structure was used for ensuring the protection at side collision for the three FPSO ships in the most exposed area namely the mooring area of the supply/transport ships.

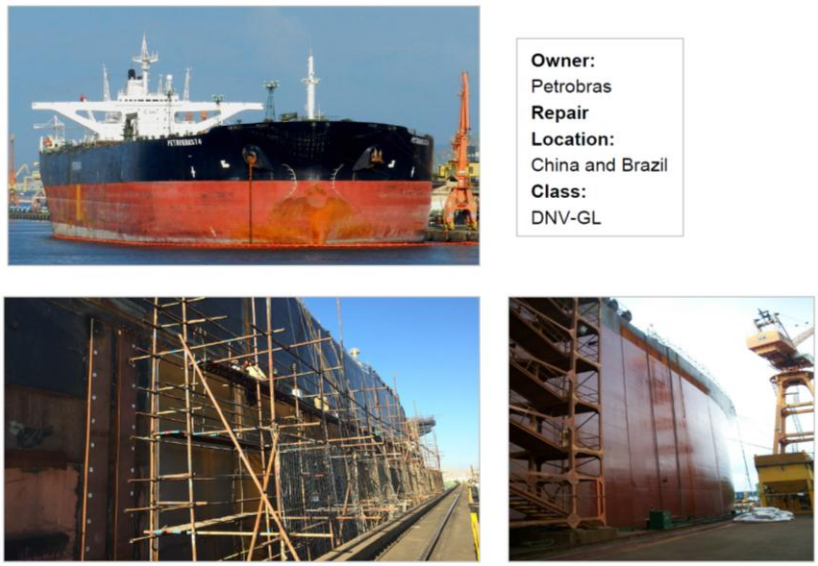

Fig.1.40 side collision protection with SPS system (IE, 2016)

The design company IE (Inteligent Engineering) has designed a Type C tanker ship for Rhin river which to comply with ADN and GL requirements. It was constructed a model also in Hanover, Germany (figure 1.41). With help of the model it was checked the process of construction and assembly, it was confirmed the quality standard of the construction and was demonstrated the simplify resulting from the usage of SPS panels.

Fig.1.41 The model of a Type C tanker ship with SPS structure (IE, 2016)

1.5 Conclusions

The necessity of the double hull structure is based on two justifications:

- satisfying the general functions (ballast and store tanks, damage stability)
- satisfying specific functions (protection of cargo tanks, ensuring smooth surfaces inside cargo hols etc etc.).

Depending the constructive particularities and the functions of every type of ship it were developed a series of classical structures of double hull, designed to meet in general the elastic behavior requirements.

In the last period it developed the plastic behavior analyze of the structures, more precisely the behavior of the structures at grounding and side collision. In this regard had appeared a series which stipulates the alayze mode for the structure and the minimal requirements to fullfill.

Therefore it developed the research of some unconventional structures which should meet both elastic behavior and requirements regarding impact strength.

CHAPTER 2
APPLICABLE RULES AND REGULATIONS

Below are presented main Rules and regulations found in ship design, which impose double hull structures.

MARPOL (MARPOL, 2006)

IMO (International Maritime Organization) das introduced in 1992, through MARPOL convention, the standards regarding the obligativity of double hull structures for oil tankers builded after 6 july 1996 (Michael G. Faure, 2006).

Thereby according MARPOL – Regulation 19, oil tankers must have double hull as follows:

- if DW < 5000 t than
  - double bottom with height h = B/15 m, but not less than 0,76 m and
  - double side with width w = (0,4 + 2,4 DW/20000) m, but not less than 0,76 m
- if DW ≥ 5000 t than
  - double bottom with height h = B/15 m, but not less than 1m and not more than 2m
  - double side with width w = (0,5 + DW/20000) m, but not < 1 m and not > 2 m

SOLAS (SOLAS, 2014)

According SOLAS, Chapter II-1, Part B-2, Regulation 9 Double bottoms in passenger ships and cargo ships other than tankers (SOLAS, 2014) – is required directly that all passenger and cargo ships to have double bottom.

MSC.235(82) - Guidelines for the design and construction of offshore supply vessels

According MSC 235(82) – Subdivision and damage stability – an offshore supply vessel must comply with the damage stability criteria in case of an side damage with 760 mm extension. Practicaly the fulfilling of this criteria is most of the time conditioned by the using of a double side structre.

IBC Code-International Code for Ships Carrying Dangerous Chemical in Bulk (IBC, 2007)

According IBC Code the ships carrying dangerous chemical in bulk classify in:

- Type 1 – outer sheell, at full load waterline, must be at a distance of not less than min(B/5, 11,5 m) from the thank walls and the bottom sheel in center line must be at a distance of not less than min(B/15, 2 m) from the bottom of the tanks and nowhere else the outer shell must be closer than 760 mm to the tanks
- Type 2 – the bottom sheel in center line must be at a distance of not less than min(B/15, 2 m) from the bottom of the tanks and nowhere else the outer shell must be closer than 760 mm to the tanks
- Type 3 – without any minimal distances.

IGC Code - International Code for Ships Carrying Liquefied Gases in Bulk (IGC, 2016)

In IGC Code is specified an important scope when designing such a structure „to ensure that cargo tanks are located in a protected location in case of a minor damage of the ship hull and that the ship can survive the damage conditions considered".

According IGC Code the ships carrying liquefied gases in bulk classify in:

- Type 1G – for substances that require maximum preventive measures against cargo loss – outer shell, at full load waterline, must be at a distance of not less than min(B/5, 11,5 m) from

the tank walls and the bottom sheel in center line must be at a distance of not less than min(B/15, 2 m) from the bottom of the tanks and nowhere else the outer shell must be closer than „d" (depending on V_c volume of each tank)

- Type 2G/2PG - for substances that require significant preventive measures against cargo loss - the bottom sheel in center line must be at a distance of not less than min(B/15, 2 m) from the bottom of the tanks and nowhere else the outer shell must be closer than „d"
- Type 3G - or substances that require moderate preventive measures against cargo loss - the bottom sheel in center line must be at a distance of not less than min(B/15, 2 m) from the bottom of the tanks and nowhere else the outer shell must be closer than „d = 0,8 m"

ADN 2017

ADN Rules, regarding the transport of dangerous goods on inland water ways, enforce the using of double side and double bottom structures in cargo area, thereby:

- Ships for transport of dry cargo – distance from outer and inner side to be of minimum 0,8 m, and height of double bottom minimum 0,5 m
- tankers, which are
    - Type G – for gases transportation – distance from outer and inner side to be of minimum 0,8 m, and height of double bottom minimum 0,6 m
    - Type C – liquid cargo – distance from outer and inner shell to be of minimum 1,0 m for structural tanks and 0,8 m for independent tanks, and height of double bottom minimum 0,6 m
    - Type N – liquid cargo – distance from outer and inner side to be of minimum 0,6 m, and height of double bottom minimum 0,5 m.

Also is permited to use alternative structures if is demonstrated by direct analyze that alternative solutions have at least the same level of safety at collision like the standard structure according ADN requirements. The criterion for evaluation of safety at collision is based on a risk analyze regarding cargo tank rupture.

NMA 123/1994

Regarding FPSO units is required in „Section 17 – Stability" that in case of an collision with a supply ship, having 5000 t displacement and 2 m/s speed, not to be produced spilling of oil from storage tanks or from processing equipments above the deck.

Conclusions

As consequence of some serious events, resulting in environmental pollution, important material damage and even loss of human lives, IMO, IACS and other authorities in the field have adopted rules regarding obilgativity and constructive measures for double hull structures.

Constructive measures imposed to double hull structures concern elastic behavior. Regarding collision behavior of ship structures, this is possible only through a direct analyze with finite element, with the help of which it can be demonstrated the efficiency of a structure in case of some collision scenarios imposed by specific rules (ADN, NMA 123/1994).

CHAPTER 3
THEOTETICAL MODELS USED FOR ANALYZE

Below are presented underlying theoretical models for calculation methodologiesof stress states in ship structures.

3.1 Theory of elasticity

Elasticity theory has as goal the determination of stress state of a continuous body, perfectly elastic, which is in equilibrium under the action of external causes.

Basic relations of elasticity theory (Ionel Chirica,1997)

The relations for solving the problems of elasticity are dividing in three categories:

a) Static ecuations

- Differential ecuations of equilibrium (Navier-Cauchy ecuations)

$$\frac{\partial \sigma_x}{\partial x} + \frac{\partial \tau_{xy}}{\partial y} + \frac{\partial \tau_{xz}}{\partial z} + g_x = 0$$
$$\frac{\partial \tau_{yx}}{\partial x} + \frac{\partial \sigma_y}{\partial y} + \frac{\partial \tau_{yz}}{\partial z} + g_y = 0$$
$$\frac{\partial \tau_{zx}}{\partial x} + \frac{\partial \tau_{zy}}{\partial y} + \frac{\partial \sigma_z}{\partial z} + g_z = 0$$

where:

g_x g_y g_z masic forces components

- Normal surface conditions v(l,m.n)

$$p_{vx} = \sigma_x l + \tau_{xy} m + \tau_{xz} n$$
$$p_{vy} = \tau_{yx} l + \sigma_y m + \tau_{yz} n$$
$$p_{vz} = \tau_{zx} l + \tau_{zy} m + \sigma_z n$$

b) Geometric ecuations

- Relation between deformations and displacements (linear expresions)

$$\varepsilon_x = \frac{\partial u}{\partial x};\ \varepsilon_y = \frac{\partial v}{\partial y};\ \varepsilon_z = \frac{\partial w}{\partial z}$$
$$\gamma_{xy} = \frac{\partial u}{\partial y} + \frac{\partial v}{\partial x};\ \gamma_{yz} = \frac{\partial v}{\partial z} + \frac{\partial w}{\partial y};\ \gamma_{zx} = \frac{\partial w}{\partial x} + \frac{\partial u}{\partial z}$$

- Continuity ecuations (Saint-Venant ecuations)

$$\frac{\partial^2 \gamma_{xy}}{\partial x \partial y} = \frac{\partial^2 \varepsilon_x}{\partial y^2} + \frac{\partial^2 \varepsilon_y}{\partial x^2};\ \frac{\partial^2 \gamma_{yz}}{\partial y \partial z} = \frac{\partial^2 \varepsilon_y}{\partial z^2} + \frac{\partial^2 \varepsilon_z}{\partial y^2};\ \frac{\partial^2 \gamma_{xz}}{\partial x \partial z} = \frac{\partial^2 \varepsilon_z}{\partial x^2} + \frac{\partial^2 \varepsilon_x}{\partial z^2}$$
$$2\frac{\partial^2 \varepsilon_x}{\partial y \partial z} = \frac{\partial}{\partial x}\left(\frac{\partial \gamma_{xy}}{\partial z} + \frac{\partial \gamma_{zy}}{\partial y} - \frac{\partial \gamma_{yz}}{\partial x}\right)$$
$$2\frac{\partial^2 \varepsilon_y}{\partial x \partial z} = \frac{\partial}{\partial y}\left(\frac{\partial \gamma_{yx}}{\partial z} + \frac{\partial \gamma_{yz}}{\partial x} - \frac{\partial \gamma_{zx}}{\partial y}\right)$$
$$2\frac{\partial^2 \varepsilon_z}{\partial x \partial y} = \frac{\partial}{\partial z}\left(\frac{\partial \gamma_{zx}}{\partial y} + \frac{\partial \gamma_{zy}}{\partial x} - \frac{\partial \gamma_{xy}}{\partial z}\right)$$

c) Fizical ecuations

- Generalized law of Hooke

$$\varepsilon_x = \frac{1}{E}\left[\sigma_x - \nu\left(\sigma_y + \sigma_z\right)\right];\ \varepsilon_y = \frac{1}{E}\left[\sigma_y - \nu(\sigma_z + \sigma_x)\right];$$

$$\varepsilon_z = \frac{1}{E}\left[\sigma_z - \nu\left(\sigma_x + \sigma_y\right)\right];\ \gamma_{xy} = \frac{\tau_{xy}}{G};\ \gamma_{yz} = \frac{\tau_{yz}}{G};\ \gamma_{zx} = \frac{\tau_{zx}}{G}$$

Potential energy of deformation (Ionel Chirica,1997)

Deformation energy accumulated in the body „U" has, in general, two effects: a variation of the volume and a variation of the shape:

$$U = U_v + U_f$$

Specific potential energy for modification of the volume

$$U_v = \frac{1-2\nu}{6E}\ (\sigma_1 + \sigma_2 + \sigma_3)^2$$

Because the potential energy for volume modification is positive, it results that v < 0,5.

Specific potential energy for modification of the shape

$$U_f = \frac{1+\nu}{6E}\ [(\sigma_1 - \sigma_2)^2 + (\sigma_2 - \sigma_3)^2 + (\sigma_3 - \sigma_1)^2]$$

Conclusion

Limits of the elasticity theory are:

- yielding of the material – exceeding of σ_c material yielding stress
- buckling – can occur in a structural element subject to compression, bending, shear or combinations of such loads, at a level of stress much smaller than σ_c. Buckling depends of geometry and loading mode of structural element and of Young's modulus.

For the alayze of structure behavior beyond this limits is used „Theory of plasticity".

3.2 Theory of plasticity

Failure criterion of the material Tresca and Mises (Jacob Lubliner, 2006)

Failure criterion is that law that define the limit of elastic behavior under the action of any possible combination of stress.

From a series of metal extrusion experiments, Tresca has concluded that failure appeared when shear maximum stress has reached a critical value. If stress vector is keept in $-\pi/6 \le \theta \le \pi/6$ sector, Tresca failure criterion can be written under this form

$$\sigma_1 - \sigma_3 = 2k \quad \sigma_1 > \sigma_2 > \sigma_3$$

Is obious that Y = 2k according Tresca failure criterion.

where: k pure shear failure stress

Y uniaxial tensile (or compression)

Von Mises suggested, from pure theoterical considerations, that failure appears when J_2 reaches a critical value. Results immediately that geometrical locus of Misses failure is a circle with radius $\sqrt{2k}$ or $\sqrt{\frac{2}{3}Y}$, and failure criterion is $J_2 = k^2$. Obvious $Y = \sqrt{3}k$ according von Mises criterion.

The two criteria have same value of Y, but value k in Mises criterion is $2/\sqrt{3}$ multiplied with value from Tresc criterion Tresca (figure 3.4).

Therefore the two geometric locus differs most in pure shear state. For most of the metals c von Mises failure criterion is preferred bacause is based on a better corelation with date from real tests.

Tresca failure criterion is a little more conservative in estimation of failure, because predicts smaller failure stress for most of the stress states.

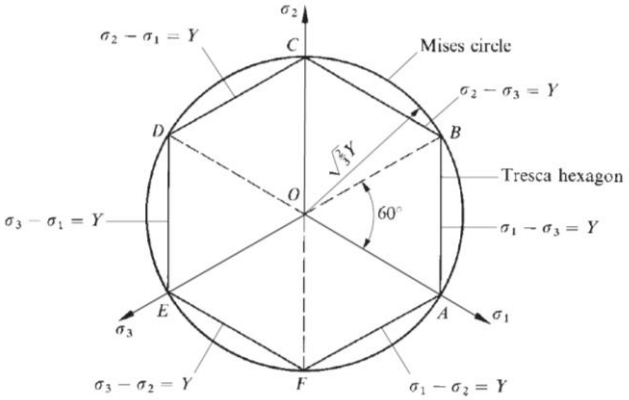

Fig.3.4 Grafic representation of Tresca and von Mises failure criteria (Chakrabarty J., 2006)

Actually, because of hardening fenomen of the material, this failure surface described above is changing (in size, center and shape).

Hardening rules depending o specific deformation (Chen W.F., 1988)

Isotropic hardening

Is supposed that the material is isotropic in normalized state and that anisotropiy and Bauschinger effect developed during cold deformation are neglected.

O formulare convenabilă din punct de vedere matematic pentru întărire este obţinută presupunând că suprafaţa de curgere se extinde uniform fără schimbarea in formă, pe masură ce starea de tensiune se schimbă de-a lungul unei traiectorii P_0P in spaţiul tensiunilor.

Kinematic hardening

This time it will be considered hardening rules that take in to account the anisotropy and the Bauschinger effect met at real materials.

An material which is initialy isotropic after failure and kinematic hardening is not any more isotropic.

It can be modeleled Bauschinger effect using mixed hardening, which is a combination of isotropic hardening and kinematic hardening.

Kinematic hardening is known by the fact that subsequent failure in compression is reduced with the same value for increasing of tensile yielding stress, in this way it is maintained al the time a difference of $2\sigma_y$ between yielding stress.

For analyze of structures behavior beyond the failurea strength of the material is used „Fracture mechanics”.

3.3 Fracture mechanics

In principle, in fracture mechanics of materials the attention is on the following aspects:

- failure energy
- macroscopic failure – trajectory and texture
- the mechanism of microscopic failure.

The strength of a given material is measured through the energy absorbed before and during the rupture process. The area under the stress-deformation curve at uniaxial tensile offers a measure of the strength. The maximum tenacity at rupture is therefore obtained with an optimum combination of strength and ductility, none high strength (for explame glass) and none exceptional ductility separately do not offers a great absorbtion of energy at rupture.

$$energie\ /\ volum\ = \int_0^{\varepsilon_f} \sigma d\varepsilon$$

Mechanism of rupture and developing of cracks at metals (E. J. Hearn, 1997)

A crack can be loaded in three different modes inside of a solid (David Broek, 1984) (figure 3.12):

- mode I – opening mode – normal stress appear. The crack surfaces are moving perpendicular on the crack plane
- mode II – sliping mode – plan shear appears. The crack surfaces are moving in the crak plane and perpendicular on the main edge
- mode III – tearing mode – out of the plane shear appears. The crack surfaces are moving in the crak plane and parallel with the main edge.

The overlapping of the three modes describes the general case of craking.

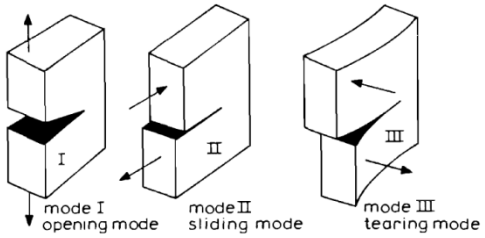

Fig.3.12 Loading modes of the cracks inside of a solid (David Broek, 1984)

Energy criterion (T.L. Anderson,1995)

For a crack with 2a length inside a infinite shell subject to a remote tensile stress (figure 14) the energy release rate is:

$$G\ = \frac{\pi\sigma^2 a}{E}$$

where: E Young's modulus
σ stress applied remote
a half of the crack length

At rupture $G=G_C$ and the above ecuation describes the critical combination of stress and crack dimension for failure:

$$G_C\ = \frac{\pi\sigma_f^2 a_c}{E}$$

Stress intensity approach

If it is supposed that the material failure at a crtical combination of stess and deformation, than results that rupture must appear at a critical intensity K_{Ic}.

For a shell, the factor of stress intensity is given by the relation:

$$G\ =\ \sigma\sqrt{\pi a}$$

The failure appears when $K_I=K_{Ic}$. In this case K_I is the driving force for rupture and K_{Ic} is a measure of the materials strength.

3.4 Methods for calculation of stress states

In the naval design practice are used in general three methods for calculation of stress states in structure elements:

a) calculation according rules of the classification society – are determined stress and deformations in structural elements calculating local and global loads based on some formulas and is verified some structural details for fatigue

b) combined calculation – with the help of FEM are determined the stress from local loads, and the stress from global loads and the fatigue check are done according the rules. This method can be applied in the case of finit element models which are extending on a limited area of the ship, for example one cargo tank/hold.

c) direct calculation – with help of FEM are determined stress from both local and global loads, and than is verified the fatigue according rules. This method is applied when finit element models are extended on full ship length or at least on three cargo tanks/holds.

Methodology of approach (Philippe Rigo, 2003)

In the initial design phase are done designing activities before receving the order. This stage is very short and represents the technical basis of the contract.

There are met three types of preliminary analizes:

1) principial methods – with help of some very simplified representation of the geometry
2) bi-dimensional geometry methods – with the help of one ore more 2D sections of the ship
3) tri-dimensionale model with coarse mesh methods – this models are used when it's needed a more detailed response. The idea is to include the principal surfaces and the actual scantling in to a 3D model which can be obtained in one or two weeks. This approach is dedicated to new concepts of ships for which there is no experience.

In detail design stage the most common structural analyze method is Finit element method (FEM). This method is very useful and can be applied to a very lwide range of analyzes: local and global strength, global and local vibration analyze, ultimate strength, detailed stress for local fatigue estimation, estimation of life cycles at fatigue, different nonlinearities analyze, collision and grounding studies.

From the calculation software suit finit element are mentioned:

- ANSYS – Ansys Inc.
- Femap – Siemens PLM Software
- Abaqus – Dassault Systemes
- CosmosWorks – SolidWorks

CHAPTER 4
PRINCIPLES IN USING NUMERICAL SIMULATIONS

4.1 Finit element method (FEM)

FEM calculation procedure according rules of the classification societies

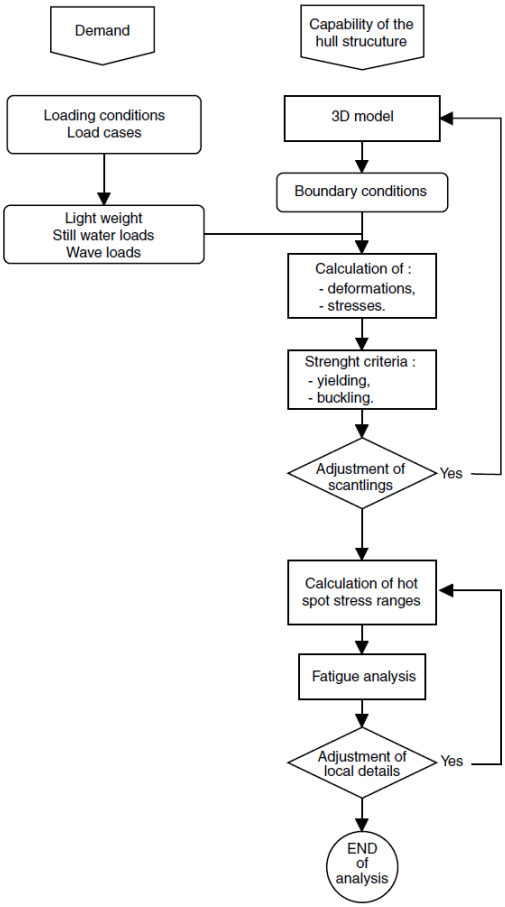

Fig.4.1 Application of FEM analyze based on tridimensional modesl **(**BV Rules, 2016)

4.2 Aspects according BV Rules, 2016 regarding application of FEM

Finit element calculations of ship structures must meet a series of requirements imposed by the classification societies rules, which refferes in general to membrane and shell element types.

Net thickness – all structural elements will be modeled with net thickness (without corrosion addition, etc.), in consequence the strength and ridigity will be reproduced according this thickness.

Model extension on longitudinal way will take into account the following:

- hull girder stress will be taken in to account corresponding
- the results from the analyzed area are not influenced by the boundary conditions

In the case of the center line symmetry the structure model can be done only on half of the ship.

Model meshing

a) coarse mesh

b) standard mesh

c) fine mesh for structural details analyze

Boundary conditions

Models which extends at least three cargo tanks/holds

Table 4.1 Symmetry and anti-symmetry in center line (BV Rules, 2016)

Boundary conditions	DISPLACEMENTS in directions **(1)**		
	X	Y	Z
Symmetry	free	fixed	free
Anti-symmetry	fixed	free	fixed

Boundary conditions	ROTATION around axes **(1)**		
	X	Y	Z
Symmetry	fixed	free	fixed
Anti-symmetry	free	fixed	free

When the hull structure is modeled on half of the ship breadth, in center line will by applied symmetry or anti-symmetry boundary conditions on as is specified in table 4.1, depending on the loads applied to the model (symmetric or anti-symmetric).

Vertical displacements will be blocked in nodes positioned at the connection of transverse bulkheads with longitudinal bulkheads, if they exist, or with the sides.

Models which extends on full length of the ship

Table 4.3 Boundary conditions to prevent the rigid body displacement of the model (BV Rules, 2016)

Boundary conditions	DISPLACEMENTS in directions **(1)**		
	X	Y	Z
One node on the fore end of the ship	free	fixed	fixed
One node on the port side shell at aft end of the ship **(2)**	fixed	free	fixed
One node on the starboard side shell at aft end of the ship **(2)**	free	fixed	fixed

Boundary conditions	ROTATION around axes **(1)**		
	X	Y	Z
One node on the fore end of the ship	free	free	free
One node on the port side shell at aft end of the ship **(2)**	free	free	free
One node on the starboard side shell at aft end of the ship **(2)**	free	free	free

When the hull structure is modeled on half of the ship breadth, in center line will by applied symmetry or anti-symmetry boundary conditions on as is specified in table 4.1, depending on the loads applied to the model (symmetric or anti-symmetric).

Loads application for the model

Local loads

- still water loads, which include:
  - sea water pressure
  - internal loads for different types of cargo and for ballast
- wave loads, which include:
  - wave pressure
  - inertial loads for different ypes of cargo and for ballast

Hull girder loads

For models which extends at least three cargo tanks/holds:

- still water and wave bending moments
- horizontal wave bending moment
- still water and wave shear forces

For models which extends on one tank/hold length it will be added to the stress obtained from local load the stress from hull girder loads.

Lightship – will be distributed on full model length, such as to obtain real longitudinal distribution of bending moments in still water.

Stress calculation

It will be calculated the following components at the centroid of each element:

- normal stresses σ_1 and σ_2 in the directions of the elelemnt co-ordinate system
- shear stress τ_{12} with respect with element co-ordinate system
- Von Mises equivalent stress

4.3 Aspects according ADN, 2017 regarding application of FEM

Boundary conditions

At both ends of the model it will blocked all three displacements. Is satisfactory the consideration of one half breadth of the model, in this situation it will be blocked transverse displacement in center line.

Meshing

The area of the structure affected during the collision must be fine enough meshed, while other area may be coarse modeled. The mesh size shall be suitable for good description of local deformations with bending and for realistic determination of elements rupture. The initiation calculation of rupture shall be based on failure criteria suitable for the type of elements used. The ratio between the long and short edge must not be more that 3. The ratio between the length and thickness of the element must be bigger than 5.

Material properties

Due to extreme behavior of the material and the structure during the collision, with nonlinear effects for both geometry and material, it must be used the real characteristic stress-deformation:

$$\sigma = C * \varepsilon^n$$

where: $n = \ln(1 + A_g)$

$$C = R_m \left(\frac{e}{n}\right)^n$$

A_g maximum elongation reported to ultimate tensile stress R_m

e natural logarithm constant

Failure criteria

The rupture of an element in FE analyze is defined by the value of failre elongation. If the calculated value of specific strain, like effective plastic strain, principal strain or, for shell elements, strain in direction of element thickness, exceeds the defined value of failure, the element must be deleted from the model and the deformation energy in this element will not modify in the next calculation steps.

CHAPTER 5
TESTE EXPERIMENTALE

5.1 Introduction

A series of experimental tests were done with the scope of validation the numerical simulation method used for analyze of double hull plastic deformation behavior. Therefore in this chapter is presented a comparison between the experiments of quasi-static plastic deformation of three types of structures and the numerical simulation of this experiments, with the scope to appreciate the approximation level of the numerical method used.

With help of this testing were obtained o series of experimental information used for verification/calibration of FEM parameters, like:

- meshing of the elements related to the thickness of the elements
- contact type between bodyes
- boundary conditions
- comparison criteria: plastic deformations and internal energy.

5.2 Preparation of experiments

5.2.1 Designing and construction of the models

For the models was used cold roller steel plate (LBR) with 1,5 mm thickness. For testing by quasi-static spherical bulb pressing were done 3 models with dimensions: 450 mm x 450 mm:

- model 1 – steel simple panel without stiffeners, thickness 1,5 mm (figure 5.3)
- model 2 – stiffned steel panel, thickness of plate and stiffeners 1,5 mm and height of the stiffeners 15 mm (figure 5.4)
- model 3 - sandwich panel made from steel-XPS polystyrene-steel, with thickness 1,5 mm x 20 mm x 1,5 mm (figure 5.5).

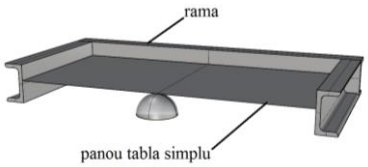

Fig.5.3– Model1

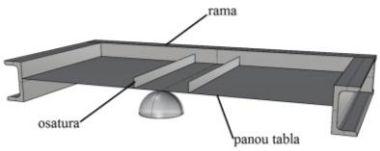

Fig.5.4–Model2

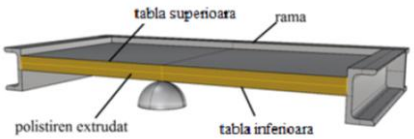

Fig.5.5–Model3

The plate panel were fixed to the frame by fillet continuous welding on the entire contour.

5.2.2 Determination of mechanical characteristics of the material used for the models.

In way to determine the material characterstic 3 test pieces were subjected to tensile test. The tensile tests of the pieces were done with the tensile testing machine from Advanced Material Research Laboratory, Faculty of Engineering from Dunărea de Jos University of Galaţi (figure 5.8).

Fig.5.8 – Tensile test

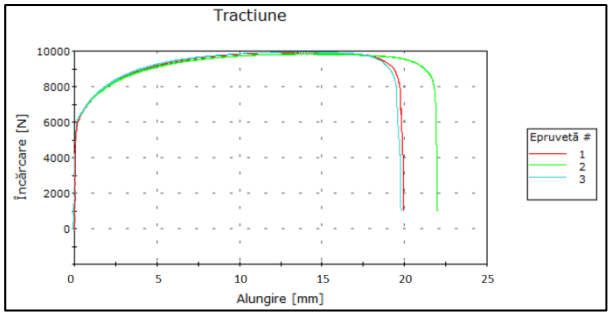

Fig.5.9 – Force-elongation diagram

In diagram from figure 5.9 are represented the curves of force-elongation for the three testing pieces.

Based on the values determined after the tensile testing of the three pieces could be established the bilinear characteritic of the material used further for numerical simulation of the model experiments, having the following characteristics (ANSYS Release 17 January 2016 – Engineering Data User's Guide):

- Young's modulus $E = 2{,}1*10^5$ MPa
- material yield stress $\sigma_c = 200$ MPa
- ultimate tensile stress $\sigma_r = 335$ MPa
- braking elongation $\varepsilon_r = 0{,}182$
- tangent modulus 745 MPa

5.2.3 Designing and construction of testing stand

In figure 5.11 is presented the assembly drawing, with the following components:

- supporting frame – overall dimensions 1400mmx720mmx540mm made from UNP80 profile
- translation mechanism with screw – M24x3 screw

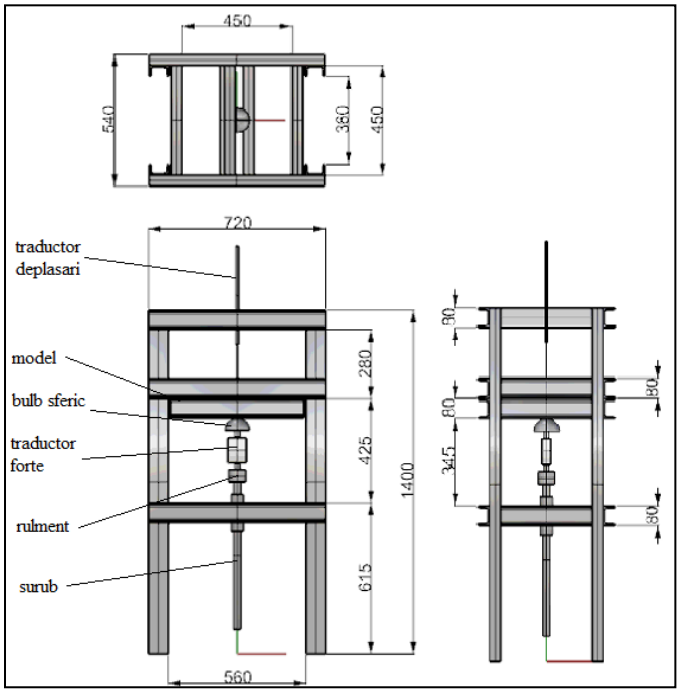

Fig.5.11 – Assembly drawing – testing stand

- bearing for eliminating the rotation of part made from force transducer-spherical bulb
- force transducer type PCL500, maximum measured force 5 kN, measuring precision ±0.5%
- displacement transducer type „inductive displacement transducer" HBM WA/300, maximum displacement measured 300 mm, precision 0.5%
- spherical bulb with ϕ60 mm diameter.

The mode of operation consists of displacement of the spherical bulb on vertical direction, perpendicular on the steel plate (of the model), measuring at predetermined intervals the acting force and the corresponding deformation of the model in the application point of the force.

Stand rigidity verification

In order to verify the influence of the stand rigidity for the precision of deformation measuring of the models, it was done an FEM analyse of the stand considering the following: vertical loading (reacting force from screw and reacting force on model frame contour = 50 kN), blocking the displacement in two of the stand legs, meshing the structure in quadratic elements with average size 10 mm.

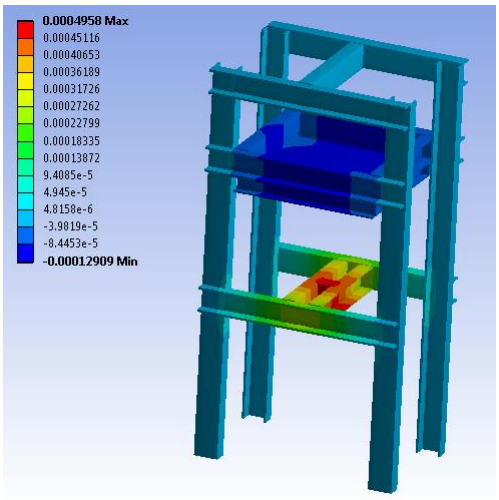

Fig.5.15 – Vertical displacements of the stand

Following the calculation resulted that vertical displacement in the middle of the model (figure 5.15) is 0,013 mm and the vertical maximum displacement of the scre support point is 0,5 mm.

Conclusion: Regarding the stand elastic deformation of 0,5 mm in the support area of the screw, because the measuring of the lower plate deformation of sandwich panel was made based on screw fillet, a correction was applied to the measured deformation of the plate. This correction is directly proportional with the applied force and has a maximum value of 0,5 mm at maximum force of 50 kN (see chapter 5.3 – 5.3.3 Experiment 3 –sandwich panel steel-XPS polystyrene-steel).

5.3 Performing experiments

5.3.1 Experiment 1 – steel simple panel

Practicaly was measured the vertical contact force between bulb and the model at every 2,5 mm vertical displacement of the bulb.

Table 5.1 – Forces and displacements – model 1

Deplasare [mm]	Forta [kN]
0.000	0.000
1.216	0.151
2.830	0.436
5.007	0.999
7.507	1.956
10.010	3.240
12.680	4.861
15.030	6.420
17.500	8.222
20.000	10.150
22.510	12.220
25.090	14.290
27.510	16.310
30.060	18.620
32.550	21.000
35.000	23.200
37.520	25.680
40.040	28.110
42.500	30.720
45.030	33.220
42.510	12.890
40.040	1.408
39.540	0.000

Table 5.2 – Internal energy - model 1

Deplasare [mm]	Forta [kN]	Energie [J]
0.000	0.000	0.000
1.216	0.151	0.092
2.830	0.436	0.566
5.007	0.999	2.128
7.507	1.956	5.822
10.010	3.240	12.324
12.680	4.861	23.139
15.030	6.420	36.394
17.500	8.222	54.477
20.000	10.150	77.442
22.510	12.220	105.517
25.090	14.290	139.715
27.510	16.310	176.741
30.060	18.620	221.276
32.550	21.000	270.603
35.000	23.200	324.748
37.520	25.680	386.337
40.040	28.110	454.112
42.500	30.720	526.473
45.030	33.220	607.357

Data recorded during the experiment are presented numerical in table 5.1 and graphicallyly in diagram from figure 5.19 below.

Integrating the force depending on displacement is obtained the curve of internal energy of the model depending on displacement (table 5.2 and figure 5.20).

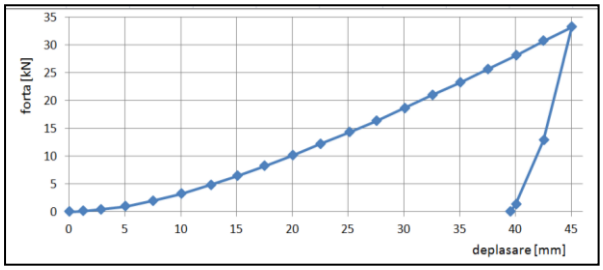

Fig.5.19–Force-displacement – model 1

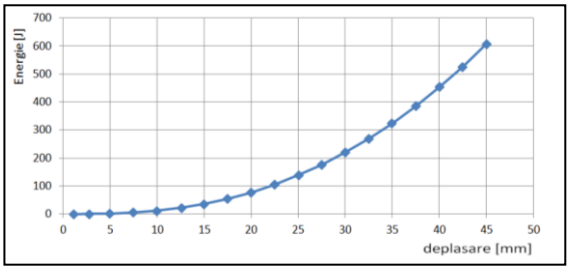

Fig.5.20–Internal energy-displacement – model 1

The shape of remanent deformation of model 1 is presented in figure 5.21 below, the left showing the lower part of the panel, the one tthat the spherical bulb acted, and the right image showing the upper part of the panel.

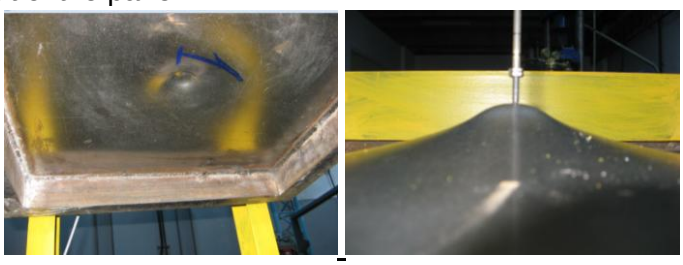

Fig.5.21 – Remanent deformation – model 1

5.3.2 Experiment 2 – steel panel with stiffener

Practicaly was measured the vertical contact force between bulb and the model at every 3 mm vertical displacement of the bulb.

Table 5.3 – Forces and displacements – model 2

Deplasare [mm]	Forta [kN]
0.000	0.000
2.841	1.615
5.768	3.410
8.666	5.440
11.570	7.600
14.460	9.817
17.370	12.230
20.270	14.700
23.190	17.330
26.080	20.010
28.990	22.700
31.890	25.500
34.810	28.500
37.680	31.370
40.530	34.600
43.460	37.700
46.350	40.640
49.220	44.000
52.140	47.000
53.970	50.950
49.550	0.000

Table 5.4 – Internal energy – model 2

Deplasare [mm]	Forta [kN]	Energie [J]
0.000	0.000	0.000
2.841	1.615	2.294
5.768	3.410	9.648
8.666	5.440	22.472
11.570	7.600	41.406
14.460	9.817	66.573
17.370	12.230	98.652
20.270	14.700	137.700
23.190	17.330	184.464
26.080	20.010	238.420
28.990	22.700	300.564
31.890	25.500	370.454
34.810	28.500	449.294
37.680	31.370	535.207
40.530	34.600	629.214
43.460	37.700	735.134
46.350	40.640	848.335
49.220	44.000	969.793
52.140	47.000	1102.653
53.970	50.950	1192.278

Data recorded during the experiment are presented numerical in table 5.3 and graphically in diagram from figure 5.23 below.

Integrating the force depending on displacement is obtained the curve of internal energy of the model depending on displacement (table 5.4 and figure 5.24).

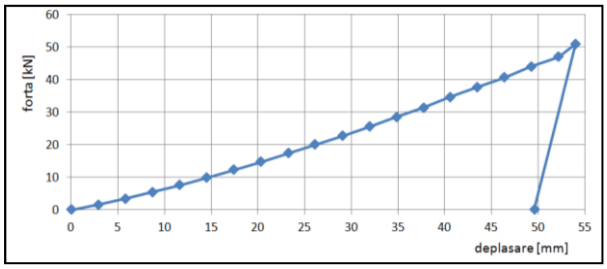

Fig.5.23–Force-displacement– model 2

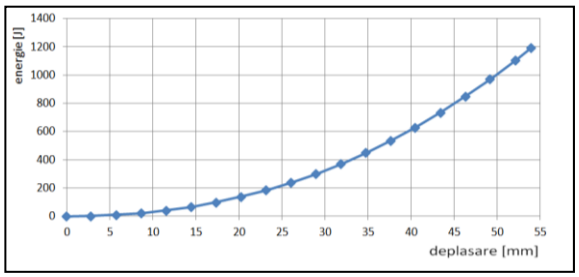

Fig.5.24–Internal energy-displacement– model 2

The shape of remanent deformation of model 2 is presented in figure 5.25 below, the left showing the lower part of the panel, the one tthat the spherical bulb acted, and the right image showing the upper part of the panel.

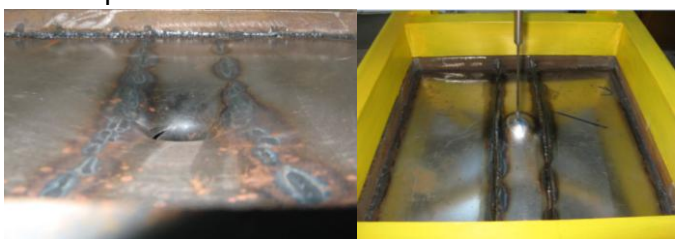

Fig.5.25 – Remanent deformation – model 2

5.3.3 Experiment 3 –sandwich panel made from steel-XPS polystyrene-steel

Practicaly was measured the vertical contact force between bulb and the model at every 3 mm vertical displacement of the bulb

Table 5.5– Forces and displacements – model 3

Deplasare inferioara masurata	Corectie def. int.	Deplasare inferioara corectata	Deplasare superioara	Forta	Distanta intre tabla inferioara si superioara
[mm]	[mm]	[mm]	[mm]	[kN]	[mm]
0	0.000	0.000	0	0	23.000
3.000	0.011	2.989	0.178	0.779	20.189
6.000	0.036	5.964	1.645	2.678	18.681
9.000	0.061	8.939	2.881	4.515	16.942
12.000	0.091	11.909	3.920	6.700	15.011
15.000	0.123	14.877	4.860	9.060	12.983
18.000	0.158	17.842	5.740	11.640	10.898
21.000	0.196	20.804	6.560	14.400	8.756
24.000	0.235	23.765	7.370	17.300	6.605
27.000	0.275	26.725	8.130	20.250	4.405
30.000	0.320	29.680	9.100	23.520	2.420
33.000	0.370	32.630	10.880	27.200	1.250
36.000	0.425	35.575	13.530	31.230	0.955
39.000	0.482	38.518	16.340	35.460	0.822
42.000	0.540	41.460	19.110	39.700	0.650
45.000	0.597	44.403	21.910	43.870	0.507
42.000	0.283	41.717	19.650	20.800	0.933
39.000	0.070	38.930	17.440	5.120	1.510
37.251	0.000	37.251	16.600	0.000	2.349

Table 5.6–Internal energy–model3

Deplasare inferioara corectata	Forta	Energie
[mm]	[kN]	[J]
0.000	0	0.000
2.989	0.779	1.164
5.964	2.678	13.152
8.939	4.515	46.794
11.909	6.700	116.633
14.877	9.060	237.972
17.842	11.640	428.394
20.804	14.400	706.644
23.765	17.300	1092.165
26.725	20.250	1603.369
29.680	23.520	2266.689
32.630	27.200	3114.108
35.575	31.230	4179.134
38.518	35.460	5492.803
41.460	39.700	7080.363
44.403	43.870	8963.778

In the case of sandwich panel were measured two displacements:

- vertical displacement of the steel plate in contact with the bulb – with help of the screw fillet (screw pitch 3mm)
- vertical displacement of the exterior plate, the one not in contact with the bulb – by displacement transducer.

Data recorded during the experiment are presented numerical in table 5.5 and graphically in diagram from figure 5.27 below.

Integrating the force depending on displacement is obtained the curve of internal energy of the model depending on displacement (table 5.6 and figure 5.28)

Because the measurement of the inferior panel deformation of sandwich panel was made based on translation of the screw, a correction was applied to the displacement of the inferior panel, directly proportional to applied force having the maximum value of 0,68 = 0,5 + 0,18 mm at maximum force of 50 kN, as following:

- 0,5 mm maximum deformation of the stand at maximum force of 50 kN (see 5.2.3)
- 0,18 mm maximum deformation of the screw at maximum force of 50 kN.

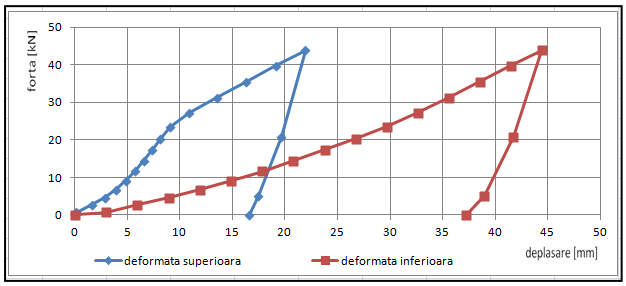

Fig.5.27– Force-displacement–model 3

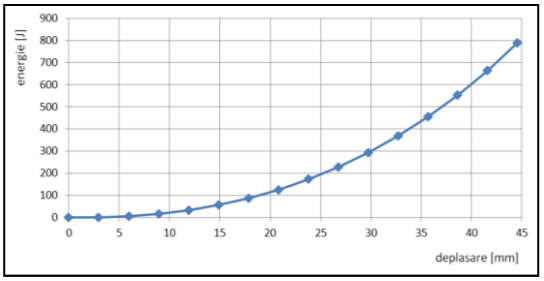

Fig.5.28–Internal energy-displacement–model 3

The shape of remanent deformation of model 3 is presented in figure 5.29 below, the left showing the lower part of the panel, the one tthat the spherical bulb acted, and the right image showing the upper part of the panel.

Fig.5.29 – Remanent deformation – model 3

5.4 Aspects regarding numerical simulations

The calculatins presented were realized using ANSYS software, Static structural module.

5.4.1 Material idealization

The material is defined by an bilinear isotropic hardening rule having Young's modulus E= $2.1 \cdot 10^5\ MPa$, yiled strength R_Y=200 MPa and tangent modulus 745 MPa (chapter 5.2.2).

5.4.2 Loading method

The loading applied to the model consists in imposing an displacement to the spherical bulb of approximativ 45 mm, normal on the surface of the plate.

The analyse timpe contains two steps:

- step 1: displacement of the bulb with 45 mm
- step 2: retraction of the bulb to initial position.

5.4.3 Finit element types

A comparison was made between the analyse with „shell" elements versus analyse with „solid" elements for model 1 – simple steel panel, considering the following aspects:

- maximum value of remanent deformation
- maximum value of equivalent stresses
- maximum value of the force in spherical bulb
- total computational time.

The calculations resulted the following values presented numerical in table 5.7 below and graphicallyly in figures 5.31 and 5.32 below:

Table 5.7 – Comparative values „shell" elements versus „solid" elements

Criteriu de comparatie	**Elemente „shell"**	**Elemente „solid"**	**Diferenta [%]**
deformata remanentă maxima [mm]	42,84	42,56	0,6
tensiune echivalentă maximă [MPa]	262,32	219,97	16,1
forţa maximă in bulbul sferic [kN]	39,393	33,630	14.6
timp total de calcul [secunde]	217	841	287

The deformation differences between the analyse with „shell" and „solid" elements are negligible, and the computation time in case of „solid" elements is almost 3 times bigger.

Conclusion: For study of unconventional structures of the double hull ships will be utilized „shell" elements meshing.

5.4.4 Boundary conditions

The boundary conditions tested on the simple panel without stiffeners, were the following:

a) fixed support on the panel contour
b) contour articulation off the steel panel
c) solid element modeling of the welding and fixed displacement and fixed rotation of the vertical side of the welding fillet
d) modeling the panel with the frame and vertical simply supporting the frame – figure 5.35

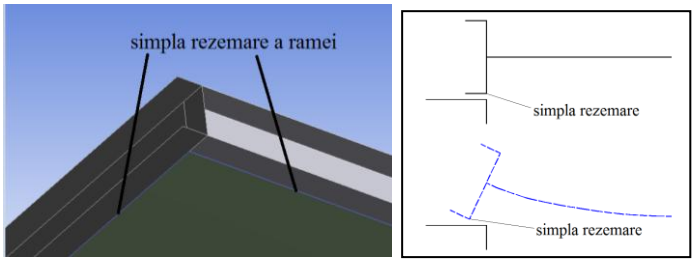

Fig.5.35 – Boundary condition d)

Table 5.8 – results for different boundary conditions

Nr.	**Situaţie**	**Deformată plastică [mm]**	**Eroare deformată[%]**	**Forţă de contact [kN]**	**Eroare forţă[%]**	**Timp de calcul [s]**
0	**Experiment**	**39.54**		**33.22**		**-**
1	a	42.836	8.3	39.393	18.6	217
2	b	42.602	7.7	39.235	18.1	251
3	c	42.560	7.6	33.630	1.2	841
4	d	40.634	2.8	25.900	-22.0	342

Analysing the results obtained for the four types of boundar conditions presented in the above table it can be resumed the following ideas:

- maximum value of the error for plastic deformation and the contact force was obtained for boundary condition a) fixed support on the panel contour
- minimum value of the error for plastic deformation and the contact force was obtained for boundary condition d) simply supporting the frame of the panel
- minimum computational time was obtained for boundary condition a) and maximum time for condition c).

Conclusion: For study of unconventional structures of double hull ships will be used and

extension of the model big enough so to unsure a minima influence of the boundary conditions.

5.4.5 Convergence test

It was realized an convergence test for 16 different meshing:

e) 8 models with uniform grid and different meshing between 2mm - 35 mm (figure 5.36 and 5.37)

f) 8 models with nonuniform grid and different meshing between 2mm - 35 mm (figure 5.38 and 5.39).

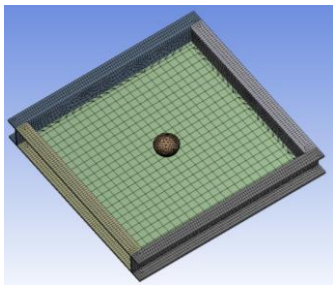

Fig.5.37 – Uniform meshing 20mm

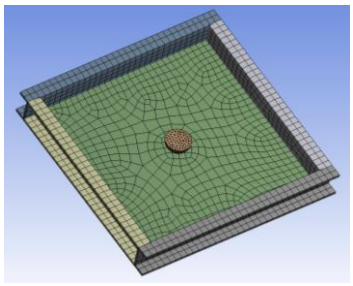

Fig.5.39 –Nonuniform meshing 20mm

Table 5.9 – uniform meshing

Nr.	Mărime element [mm]	Deformată plastică [mm]	Eroare deformată[%]	Forţă de contact[kN]	Eroare forţă[%]	Timp de calcul [s]
0	**Experiment**	**39.54**		**33.22**		**-**
1	2	40.667	2.9	25.669	-22.7	2385
2	5	40.634	2.8	25.900	-22.0	342
3	10	40.538	2.5	26.916	-19.0	113
4	15	42.857	8.4	27.989	-15.7	110
5	20	40.691	2.9	29.202	-12.1	97
6	25	43.328	9.6	29.448	-11.4	73
7	30	41.081	3.9	33.265	0.1	98
8	35	41.243	4.3	35.008	5.4	79

Table 5.10 – nonuniform meshing

Nr.	Mărime element[mm]	Deformată plastică[mm]	Eroare deformată[%]	Forţă de contact[kN]	Eroare forţă[%]	Timp de calcul[s]
0	**experiment**	**39.54**		**33.22**		**-**
1	2	40.703	2.9	26.455	-20.4	176
2	5	41.114	4.0	26.692	-19.7	97
3	10	41.108	4.0	27.069	-18.5	58
4	15	42.107	6.5	27.209	-18.1	67
5	20	41.772	5.6	27.952	-15.9	55
6	25	41.986	6.2	29.500	-11.2	48
7	30	42.754	8.1	28.670	-13.7	60
8	35	41.902	6.0	31.481	-5.2	71

The results presented in table 5.9 and table 5.10 aboe show that for:

g) uniform grid 10 mm meshing provides an error of 2,5% for deformation, 19,0% for contact force and an computational time of 113 s.

h) nonuniform grid 20 mm meshing provides an error of 4,0% for deformation, 18,5% for contact force and an computational time of 58 s.

The contact force differences are bigger, partially because of the approximation of the material characteristic with an bilinear rule.

Conclusion: For study of unconventional structures of double hull ships will be used an nonuniform grid meshing, for reducing the computational time, respecting the value of the ratio element length/element thickness = 7 in the area of interest.

5.5 Comparative analyze experiment-numerical simulation

5.5.1 Example 1 – simple steel panel

In figures 5.44 and 5.45 below are presented in comparison the diagrams for force-displacement and internal energy-displacement for numerical simulation and the experiment.

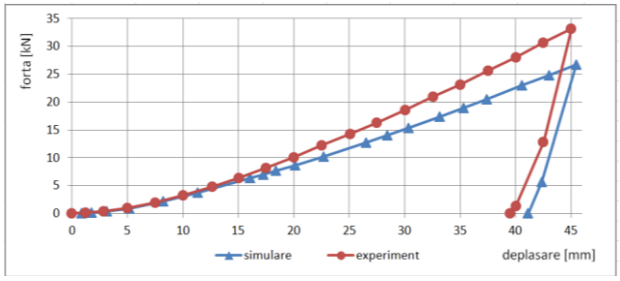

Fig.5.44–Force-displacement model1

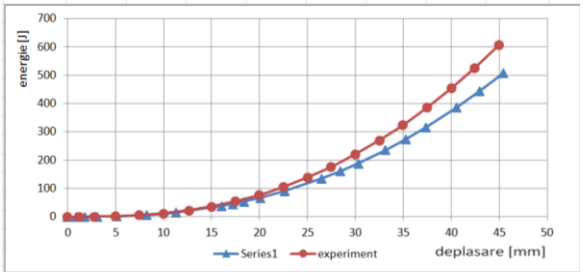

Fig.5.45–Internal energy-displacement model1

5.5.2 Example 2 – stiffened steel panel

In figurile 5.51 and 5.52 below are presented in comparison the diagrams for force-displacement and internal energy-displacement for numerical simulation and the experiment.

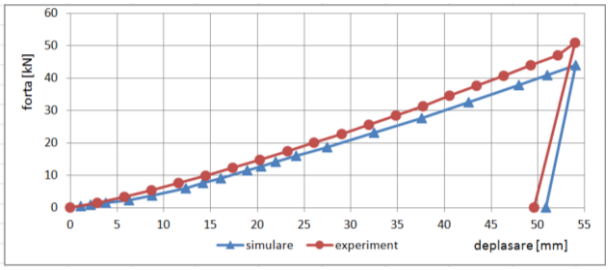

Fig.5.51– Force-displacement 2

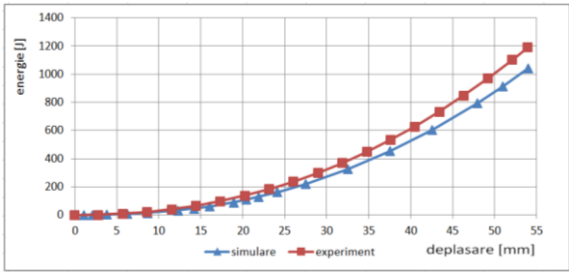

Fig.5.52– Internal energy-displacement model 2

5.5.3 Example 3 – sandwich panel from steel- XPS polystyrene-steel

In figures 5.57 and 5.58 below are presented in comparison the diagrams for force-displacement and internal energy-displacement for numerical simulation and the experiment.

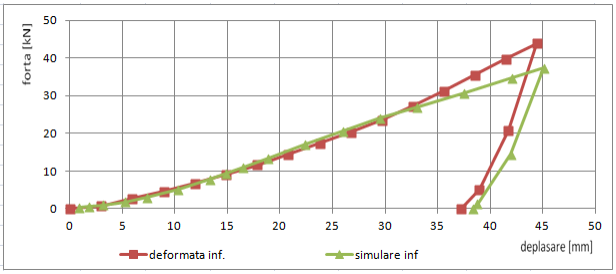

Fig.5.57– Force-displacement model 3

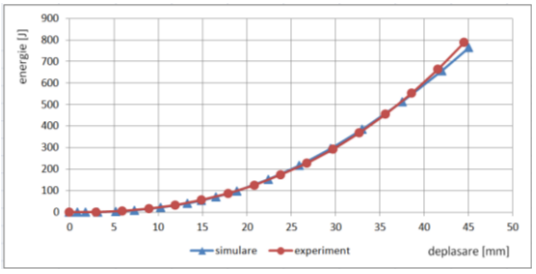

Fig.5.58– Internal energy-displacement model 3

5.6 Conclusions

The results of comparative analyse are presented in table 5.11 below:

Table 5.11 – comparative centralizer experiments-simulations

		Diferente [%]		
Nr.	**Experiment**	**Deformată plastică**	**Forţă de contact maximă**	**Energie internă**
1	**Experiment 1**	4.0	-18.5	16.43
2	**Experiment 2**	2.70	13.79	12.51
3	**Experiment 3**	2.86	14.93	3.13

It can be observed that maximum difference for plastic deformation between the experiments and numerical simulations is of maximum 4%.

Considering the safety margin used in the field of naval structures, in general between 5% and 10%, it can be concluded that the error level beteen the realized experiments and the afferent numerical simulations is falling in to the accepted error margin.

CHAPTER 6
ANALYZE OF CONVENTIONAL STRUCTURE OF DOUBLE SIDE

6.1 Description of conventional double side structure

Conventional structures analysed, for comparison with unconventional strctures, is a cargo hold from the middle part of an inland vessel provided with double side and double bottom.

Considered vessel is a tanker selfpropelled ship with structural tanks, for transportation on inland waterways of dangerous goods like: gasoline, products with >10% benzene, clorbenzene, heptanes, octane etc.

Ship principal characteristics:

Length overall	99,90 m
Breadth	9,45 m
Depth	4,75 m
Draft (scantling)	3,20 m
C_B	0,9
Frame distance	625 mm
Web frame distance	1875 mm

Conventional structure analysed is provided with double side of 0,8m width and double bottom of 0,7m height in center line and 0,9 m at double side, ensuring practically for cargo area an ratio volme of cargo tanks/total volume = 70%.

Considered structure for analyse is formed from a central tank between frames C93-C111, half of tank at aft, from frame C85 at C93, and half of tank at fore from C111 at C119 (figure 6.1).

Deck, bottom and double bottom, side and double side structures are in longitudinal framing system, otherwise are provided simple frames on the side at every 625 mm and web frames on all structures at every 1875 mm.

In figures 6.2 - 6.6 are presented an overview of the structures and also every type of frame of the structure.

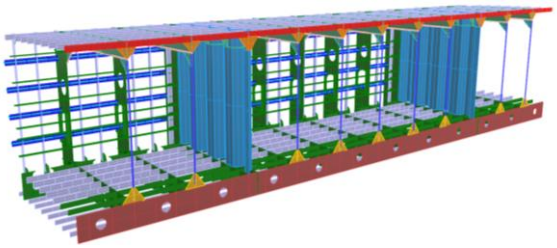

Fig.6.3 – Model 3D – without the shells

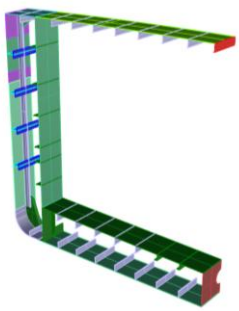

Fig.6.4–Simple frame

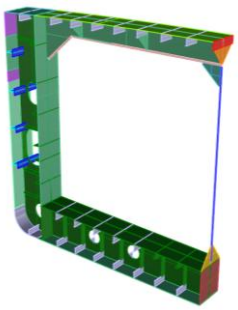

Fig.6.5–Web frame

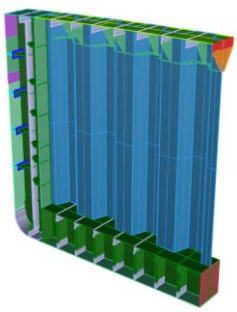

Fig.6.6-Watertight bulkhead

In calculation were used net thickness of the structure elements.

To verify the strength of the structure in elastic behavior a finit element analyse was made in middle area in chapter 6.2 below.

In order to compare the capacity of absorbtion of impact energy, in collision situation, of the conventional structure compared with different unconventional structures, a finit element analyse was realized in plastic deformation with an quasi-static loading in chapter 6.3 and with an dynamic loading in chapter 6.4 for the conventional structure.

6.2 Analyze of conventional structure in elastic behavior

Considered structure for elastic behavior analyse is represented by central area tanks between frames C85-C119, having the components presented in table 6.1. The analyse was made in ANSYS with Static Structural module.

6.2.1 Model meshng

The model was meshed in quadratic elements type „quad4", having average size of 50 mm.

In figure 6.7 is represented the meshing of the structure elements.

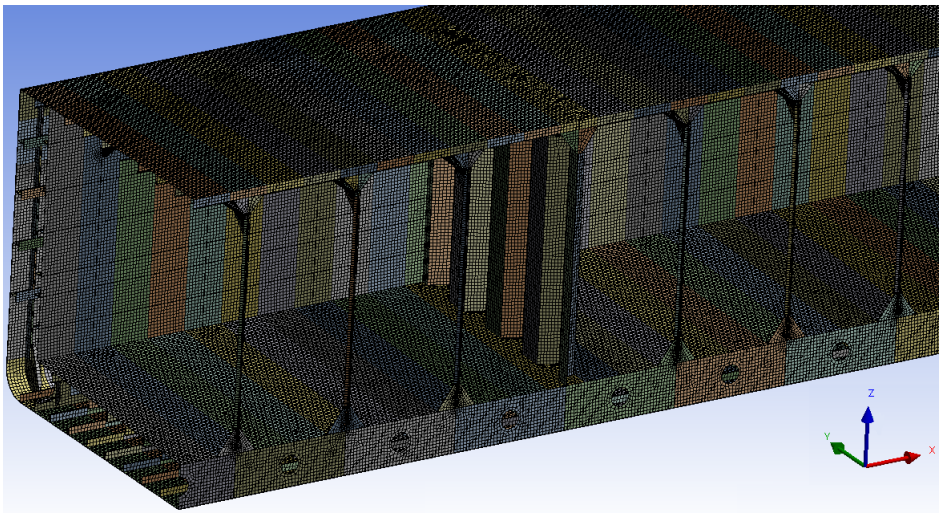

Fig.6.7 – Conventional structure meshing

6.2.2 Material

The material used for analyse is S235 steel, with admissible equivalent stress values of:

$$\sigma_{VM} = \frac{0.98 \cdot R_Y}{\gamma_R} = \frac{0.98 \cdot 235}{1.05} = 219.3MPa$$

6.2.3 Boundary conditions

According BV Rules, 2014 the following boundary conditions were used:

- symmetry conditions at aft and fore extremities of the modes
- fixed vertical displacements in nodes situated at the connection of the transverse bulkheads C93 and C111 with double side situated at Y = 3,925 m from center line
- symmetry conditions in center line

6.2.4 Model loadings

6.2.4.1 Local loadings-The following loading cases were anlysed:

A) Full load:

- structure own weight
- external pressure of the water on the shell in two situations:
  - A1 – maximum draught 3,2 m plus wave crest 0,6 m = 3,8 m free surface height
  - A2 – maximum draught 3,2 m minus wave trough -0,6 m = 2,6 m free surface height
- internal pressure from liquid cargo on double side and double bottom – it was considered the maximum level of cargo tank filling 4,7 m from the base line and a 0,89 t/m^3 cargo liquid density.

B) Ballast:

- structure own weight

- external pressure of the water on the shell in two situatins:
  - B1 – minimum draught 2,0 m plus wave crest 0,6 m = 2,6 m free surface height
  - B2 – minimum raught 2,0 m minus wave trough -0,6 m = 1,4 m free surface height
- Internal pressure from ballast on side and double side, bottom and double bottom – it was considered the maximum filling level of ballast tanks 4,7m from the base line and a 1,0 t/m^3 ballast water density (figure 6.11).

6.2.4.2 Longitudinal bending of the hull girder stresses

The stresses from longitudinal bending were determined as follows:

$$\sigma_{HGL} = \frac{MAX\left(\left|M_H\right|,\left|M_S\right|\right)+\left|M_{AD}\right|}{Z}\cdot 10^3\ [MPa]$$

M_H, M_S = admisibile bending moment in hog and sag in calm water

M_{AD} = additional bending moment depending on the navigation area

Z = net ship section modulus [cm^3]

6.2.5 Calculation results

The calculation of total stresses in structure elements of double side was done by summing up the maximum values of stresses from ,ocal loads σ_{FEM} (6.2.4.1) and from hull girder loads σ_{HGL} (6.2.4.2): $\sigma_{TOTAL} = \left|\sigma_{FEM}\right| + \left|\sigma_{HGL}\right|$.

In table 6.4 below was considered the maximum value of stress σ_{FEM} resulted from the four loading cases analysed (A1, A2, B1 and B2) for every structure element.

Table 6.4 – conventional double side stress level

Nr.	**Denumire element**	**z**	**Z**	**σ_{HGL}**	**σ_{FEM}**	**σtotal**
		[m]	[cm3]	[MPa]	[MPa]	[MPa]
2	Tablă lacrimară	4.79	659714	54	12	66
3	Centură	4.758	667970	53	12	65
4	Tablă bordaj 1	4.2	854427	41	11	52
5	Tablă bordaj 2	3.57	1247626	28	38	66
6	Tablă bordaj 3	3.3	1554140	23	83	106
7	Tablă gurnă	0	776011	45	48	93
9	Tablă dublu bord	4.79	659714	54	79	133
12	Diafragmă bordaj etanşă				24	24
14	Diafragmă bordaj				112	112
17	Coastă simplă bordaj HP160x7				45	45
18	Brachet gurnă				37	37
19	Longitudinale punte HP140x7	4.79	659714	54	17	71
21	Stringheri bordaj inimă 160x10	3.97	965517	37	39	76
22	Stringheri bordaj platbandă	4.04	928766	38	37	75
23	Longitudinale fund HP 120x7	0	776011	45	37	82
24	Longitudinale dublu bord HP	4.2	854427	41	117	158
29	Curent lateral Y3925	0	776011	45	36	81
31	Nervuri diafragmă bordaj 100x8				69	69
40	Bracheţi diafragmă bordaj etanşă				85	85

Conclusion: From table 6.4 above results that stress values are under the admissible values σ_{VM} = 219,3 MPa.

In figure 6.12...6.15 are represented the distribution of stresses and the deformation of the structure under the local loads.

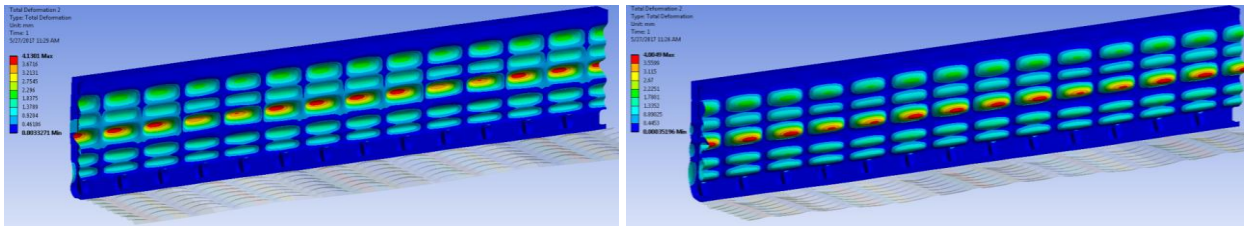

Fig.6.14 – conventional double side deformation – loading case A2 and B1

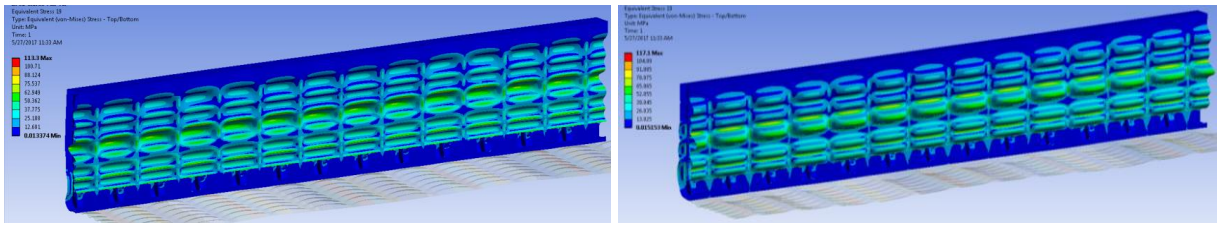

Fig.6.15 – Conventional double side stress distribution – loading case A2 and B1

6.3 Analyze of conventional structure in plastic behavior with quasi-static load

In order to evaluate the behavior of the conventional double side structure in collision situation, a finit element analyse was done in plastic deformation behavior, considering a quasi-static loading with an bow model of inland barge, according ADN, 2017 (figure 6.16).

The calculation was performed in ANSYS-Static Structural modulus.

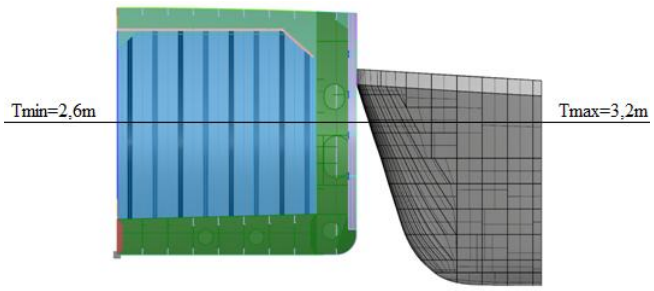

Fig.6.16–Relativ position

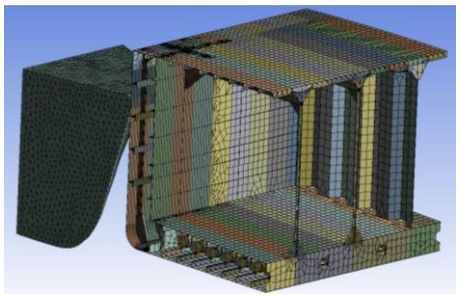

Fig.6.17–Structure meshing

For plastic deformation analyse the symmetry condition against the center line of the bow model was used, so was modeled only half of the striking bow and from the central area of the conventional structure.

6.3.1 Model meshing

The model was meshed with quadratic elements type „quad4”, having the average size of 25 mm in the contact area between the bow and the side and average size of 200 mm for the rest of the structure.

In figure 6.17 is represented the meshing of the structure elements.

6.3.2 Material

For plastic deformation analyse was used as material for the conventional structure S235 steel, having the following characteristics according DNV RP-C208, 2013: Young’s modulus E = 2,1 x 10^5 MPa, yielding stress R_Y = 236.2 MPa, tangent modulus 1105 MPa, Poisson ratio 0,3.

6.3.3 Boundary conditions

According BV Rules, 2014 and ADN, 2017 were used the following boundary conditions:

- all three displacements fixed at fore end of the structure model
- symmetry conditions in transversal plane at C103+312.5
- symmetry conditions in center line

The friction between the bow and the side was considered with constant friction coefficient μ=0,3.

6.3.4 Model loading

For conventional structure analyse at plastic deformations was imposed an quasi-static displacement in transverse way to the bow model, perpendicular to the center line of the structure model.

The analyse time contents two steps:

- step 1: maximum transverse displacement of 0,79 m
- step 2: retraction of the bow in the initial position.

It was considered maximum transverse displacement of 0,79 m according ADN, 2017.

6.3.5 Calculation results

In figure 6.19 is represented remanent deformation of the conventional structure model.
In figure 6.20 is represented the stress distribution in conventional structure at the end.

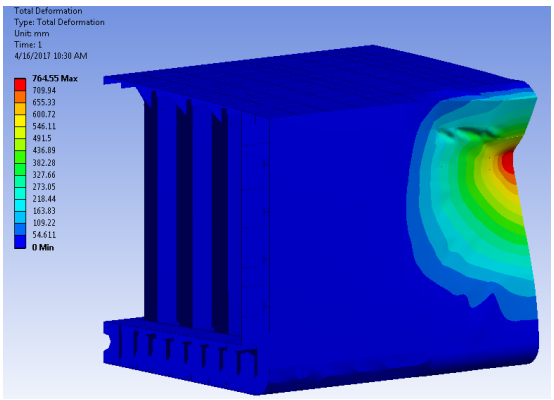

Fig.6.19–Remanent deformation

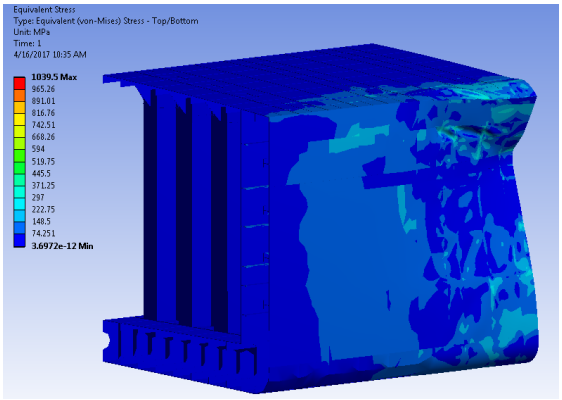

Fig.6.20–Stress distribution at quasi-static load

In figure 6.21 is represented the contact force diagram, exporessed in kN, depending on the bow model displacement, expressed in m.

In figure 6.22 is represented the internal energy diagram, expressed in J, depending on the bow model displacement, expressed in m.

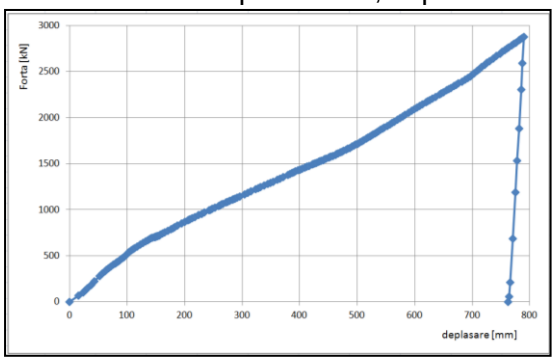

Fig.6.21–Contact force-displacement

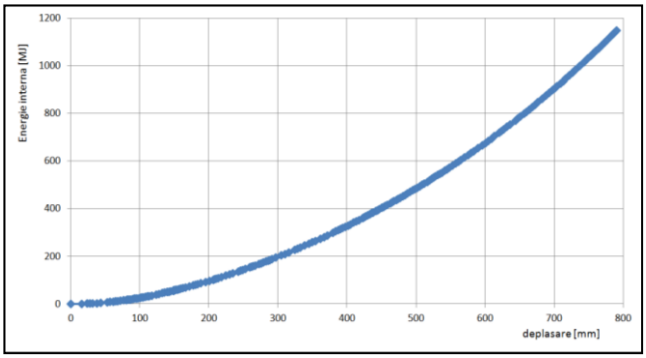

Fig.6.22–Internal energy-displacement

6.4 Analyze of conventional structure in plastic behavior with dynamic load

In order to appreciate the behavior of the double side structure in situation of an collision considering the material failure, a finit element analyse was done with plastic deformation in ANSYS-Explicit Dynamics (ANSYS Release 17 January 2016 – ANSYS Explicit Dynamics Analysis Guide).

Remark: According ADN, 2017 requirements the appreciation criteria of ship structure strength at collision with another ship is the energy absorbed by the structure until the moment of the failure of the carg tank walls.

6.4.1 Model meshing

For a reasonable computational time, was used an meshing in quadratic elements type „quad4”, having average size of 50 mm in the contact area of the bow and the side and 200 mm

for the rest of the strcuture.

6.4.2 Material

For plastic deformation analyse with dynamic loading same material as in 6.3.2 was used.

Additional, it was used as failure criterion for the material the specific strain ε_k = 0,171, determined according (Peschmann, 2000).

6.4.3 Boundary conditions

Were applied the boundary conditions from chapter 6.3.3.

It was considered the friction between the bow and the side, using an dynamic friction coefficient according (ADN, 2017).

6.4.4 Model loading

For the analyse of the plastic-dynamic deformation was imposed an initial kinetic energy to the bow model through:

- initial speed 4 m/s on transverse direction, direction Oy
- bow model weight 750 t

6.4.5 Calculation results

6.4.5.1 Global deformation

In figures 6.24 and 6.25 is presented the remanent deformation of the conventional structure at scale 1:1.

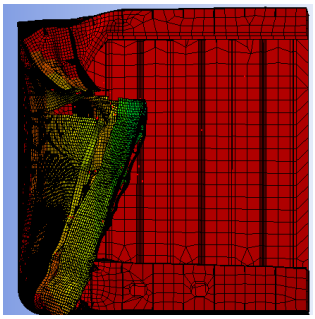

Fig.6.24 – Remanent deformation-transversal

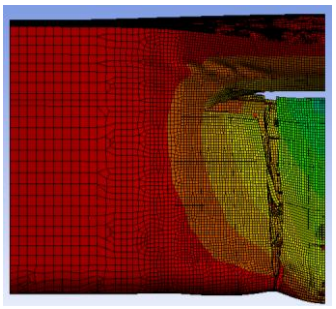

Fig.6.25–Remanent deformation-longitudinal

6.4.5.2 Double side rupture

Durring the calculation, the program register the deterioration level of the mesh elements depending on time, showing the results on a scale from 1 to 4 thereby: 1 –elastic, 2-plastic, 3-partial failure and 4- final failure accordin the given failure criterion. Thus, based on this results it can be determined when and where appeared the failure of the structure elements.

In figure 6.26 below is presented in left side the situation at t = 0,43 s when first elements of the tank shell have failed and in the right the moment t = 1 s at the final of the collision.

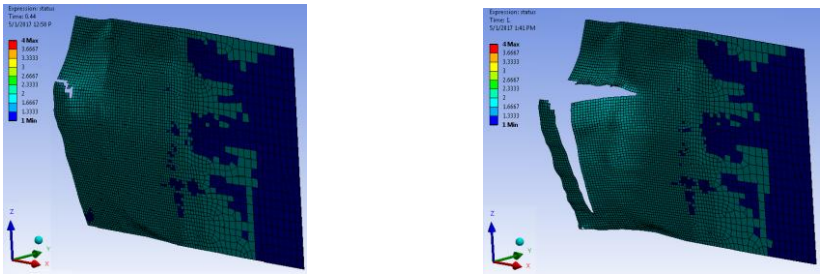

Fig.6.26 – Failure of the tank shell – conventional structure

It were identified the following causes of the inner hull failure:

- the failure of the elements in a horizontal plane corresponding to the bow model deck and situated in close proximity of one double side longitudinal stiffener, at moment t = 0,43 s

- failure of the elements on a vertical direction because the contact area between the simple frame of the outer shell, HP 160 x 7 profile, and the sinner side shell, at moment t = 0,45 s.

In figures 6.27 and 6,28 is presented the evolution of the two ruptures, horizontal and vertical, in a view from the interior of the tank to the double side, respectively in a view from the exterior of the tank to the outer side. It can be observed the local areas highly stressed which yields at an further time step.

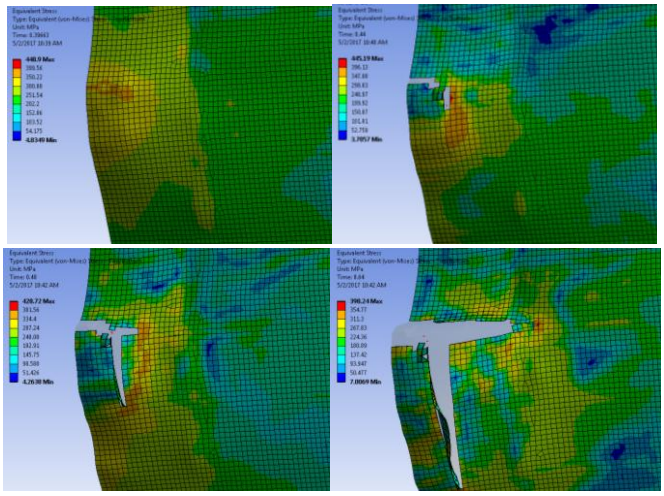

Fig.6.27 – Failure of the tank shell – conventional structure

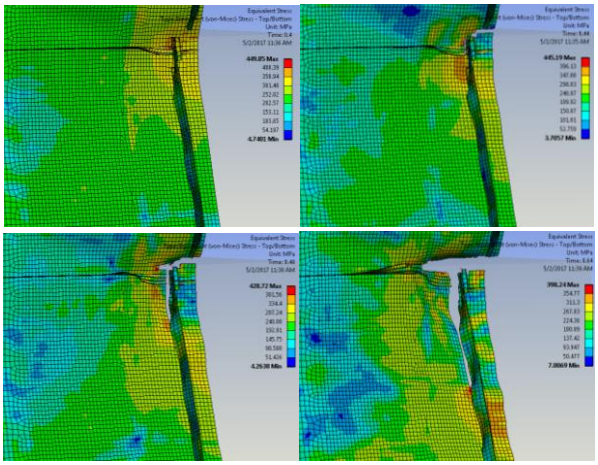

Fig.6.28 – Contact area outer side frame and the inner side shell– conventional structure

6.4.5.3 Deformation energy in the structure elements

In figure 6.29 it can be observed that deck web frame, double bottom floor and lateral double bottom floor, situated in continuity of doble side, presents the smallest deformation energy, so they have a minimum contribution to the energy absorbtion during the collision.

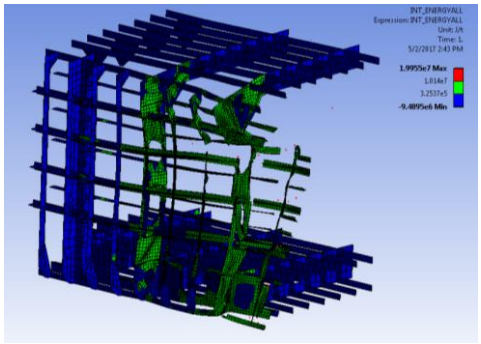

Fig.6.29 – Deformation energy in the structure elements – conventional structure

6.4.5.4 Local deformations

Analyzing the deformations map of the structure was found the following trends in conventional structure deformation during the collision:

- deck bending and the roation of the ensemble deck-side and deck-double side – figure 6.30

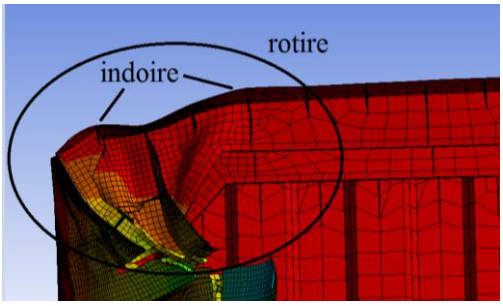

Fig.6.30–Deck bending and deck-side rotation

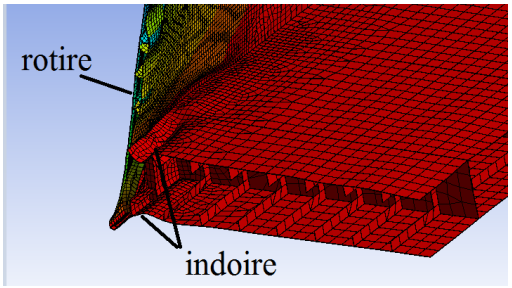

Fig.6.31–Bottom and double bottom bending and side rotation

- bottom and double bottom bending and side structure and double side rotation – figure 6.31
- bending and rupture of the side web frame and outer side stiffeners – figure 6.32

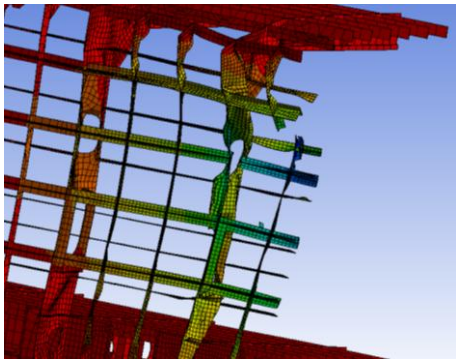

Fig.6.32 – Bending and rupture web frame and stiffeners of outer side

6.4.5.5 Energy and displacements depending on time

In figure 6.33 is presented kinetic energy diagram [MJ] of the bow model depending on time.

It is observed that bow model kinetic energy from the start of the simulation ($m * v^2)/2$ = (750 t * (4 m/s) ^{2})/2 = 6 [MJ], is transferred to the structure model in two stages:

- first stage, in time interval 0 – 0,5 s, when the gradient of energy decreasing is big
- second stage, in interval 0,5 – 1 s, with a smaller energy decrease radient, when practical is consumed only approximativ 25% from the total energy.

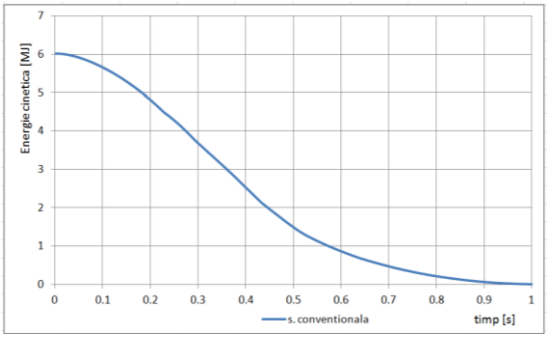

Fig.6.33 – Kinetic energy diagram – conventional structure

In figure 6.34 is presented the internal energy diamgram [MJ] of structure model depending on time.

In this case also it can be noted the same differentiation in two stages: first stage (0 – 0,5 s) when is developed the most of thedeformation energy and the second stage (0,5 – 1 s) when the energy variation in time is slower.

In figure 6.35 is presented the bow model displacement diagram [m] in Oy direction of the structure model depending on time.

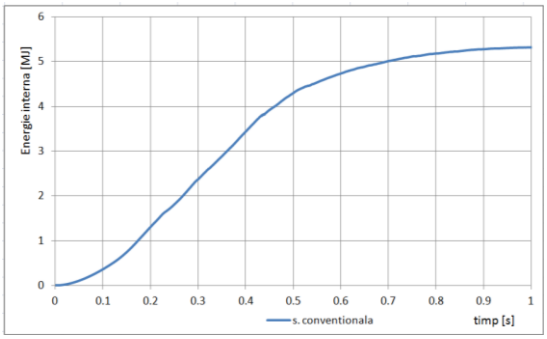

Fig.6.34–Internal energy

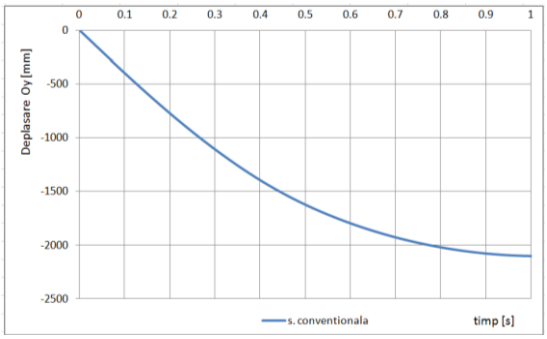

Fig.6.35–Bow displacement

It can be observed a strong deceleration in first stage (0 – 0,5 s) of the impact, corresponding to the rapid growing of deformation energy, followed by a slower braking of the bow model in the second stage.

Conclusions In table 6.7 are presented the values of internal total absorbed energy of the structure during the impact, the time moment when appeared the failure of the double hull shell, the deformation energy registered until the failure of tank shell and the total displacement of bow model until the final of the collision (the moment when kinetic energy becomes zero).

Table 6.7 – conventional structure results centralizing

Structure	Energie internă totală [MJ]	Moment cedare dublu bordaj [s]	Energie internă la cedare dublu bordaj [MJ]	Deplasare maximă prova [m]
Structure conv.	5.318	0.44	3.830	-2.100

Analyzing the results obtained for conventional structure the following conclusion were drawn:

a) to be avoided using stiffeners on the oute side which can become stress concentrators at the contact with the inner side shell, thus leading to failure of the last one (see 6.4.5.2),

b) to be avoided using at inner side of elements with great stiffness differences in OY direction, the deformation direction imposed by bow model (see 6.4.5.2),

c) considering the deformation energy it can be appreciated the level of participation for every structure element durring the impact and it can be redesigned the structure such that results a weight reduction simultaneous with a similar energy absorbtion capacity (see 6.4.5.3),

d) analyzing the local behavior of structure elements it can be identified different solution for increasing the level of total energy absorbtion of structure during the collision (see 6.4.5.4)

e) correlating the kinetic/internal energy and displacement diagram depending on time with the deformation maps it can be established the efficiency of different solutions for unconventional structures (see 6.4.5.5).

Remark In the following it will be investigated different types of unconventional structures in order to obtain an response to the problemes identified at conventional structure, having as final purpose a deformation energy as big as possible until the moment of double side rupture with as small as possible weight of the structure.

CHAPTER 7
INVESTIGATION OF SOLUTIONS FOR UNCONVENTIONAL STRUCTURES

Strategy

Analyzing the deformation mode of conventional structure at collision, the areas in which appear stress concentrators, the failure mode of tank shell were identified the following solutions to be investigated:

- using some structure elements which to transmit the energy from highly loaded zones to less loaded zones – **structure „K”** (TYPE1)
- using of some elements which to dissipate the stress concentrators that leads to material failure – **structure „SANDWICH”** (TYPE2, TYPE3, TYPE4)
- reinforcing the outer side – **structure „ICE”** (TYPE5)
- using a more ductil material at inner side shell – **structure „DUCTIL”** (TYPE6)
- reducing the weight of structure elements with low participation to deformation energy – **structure „LIGHT”** (TYPE7)
- reinforcing of the inner side – **structure „ARC”** (TYPE8).

For every type of solution was analysed the feasibility and were identified the principal aspects regarding the implementation in naval construction. Thus, were considered:

- variations of the proposed structure compared to conventional structure
- accessibility of the proposed materials for ship industry
- structure construction technology
- ADN 2017 requirement regarding the adjacent spaces of the cargo tanks which must be inspectable and cleaned, so practical double side and double bottom spaces must be provided with passing holes of at least 0,36m^2 and a minmum width of at least de 0,5 m.

In order to realize the comparative analyse of unconventional structures were considered the following appreciation criteria:

- performances until the final of the collision
  - total internal energy
  - total penetration distance
- performances until the moment of tank shell failure
  - partial internal energy
  - partial penetration distance
- structure weight
- ratio between internal energy/structure weight.

7.1 Unconventional structure of double side „K” - TYPE1

7.1.1 Structure description TYPE1

Structure TYPE1 consists in adding to conventional structure of the following elements at simple frame (figure 7.1.1):

- deformable girder: long girder „I” section profile 115x8/100x8 mm and short girder „I” section profile 125x8/100x8 mm,
- FB 100x8 at simple frame
- bracket between deck and double side, inside double side 480x260x6,5 mm
- bracket between deck and double side, inside cargo tank 800x425x6,5 mm with flange 40x6,5 mm and FB in the continuation of the bracket for stiffening deck shell 1000x140x6,5mm

- bilge bracket 6,4 mm thickness with flange 100x6,4 mm and FB in continuation of the bracket for stiffening bottom shell 425x120x6,4mm
- double bottom bracket 680x425x6,5 mm with flange 40x6,5 mm and FB in continuation of bracket for stiffening of the double bottom shell 1000x160x6,5mm
- bracket double side-double bottom 710x425x6,5 mm with flange and intermediate stiffener 40x6,5 mm

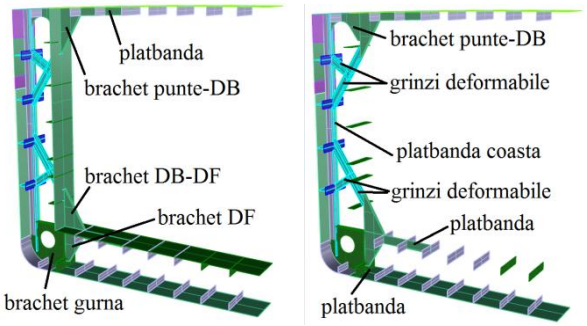

7.1.3 Structure analyse TYPE1 in plastic deformation with dynamic load

Table 7.1.1 –structure TYPE1 results centralizing - total

Structure	Energie internă totală	Diferenţă Energie internă totală	Deplasare maximă	Diferenţă Deplasare maximă	Masă	Diferenţă masă	Energie internă totală/masă structure
	[MJ]	%	[m]	%	[t]	%	[MJ / t]
Structure conv.	5.318	-	-2.100	-	11,88	-	0,448
K-TYPE1	5.148	-3,2%	-1.705	-18,8%	12,84	8,1%	0,401

Table 7.1.2 –structure TYPE1 results centralizing - rupere

Structure	Moment rupere dublu bordaj	Energie internă rupere	Diferenţă Energie internă rupere	Deplasare până la rupere	Diferenţă Deplasare până la rupere	Energie internă rupere/masă structure
	[s]	[MJ]	%	[m]	%	[MJ / t]
Structure conv.	0.440	3.830	-	-1.410	-	0,322
K-TYPE1	0.462	4.330	13,1%	-1.444	2,4%	0,337

7.2 Unconventional structure of double side „SANDWICH” - TYPE2

7.2.1 Structure description TYPE2

Structure TYPE2 consists in adding to conventional structure of the following elements (figure 7.2.1):

- one layer of polystyrene 160 mm thick on the outer side shell,
- one layer of steel 4 mm thick applied over the polystyrene of outer side, such that it results an sandwich shell for the outes side made from steel-polystyrene-steel
- one layer of polystyrene 140 mm thick on the inner side shell,
- one layer of steel 4 mm thick applied over the polystyrene of inner side, such that it results an sandwich shell for the inner side made from steel-polystyrene-steel.

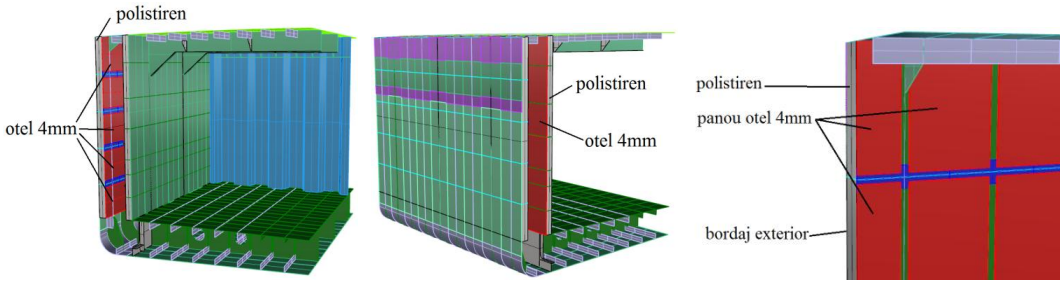

Fig.7.2.1 – Model 3D – structure TYPE2

7.2.3 Structure analyse TYPE2 in plastic deformation with dynamic load

In table 7.2.1 are presented comparative between the conventional structure, structure TYPE1 and structure TYPE2, results obtained until the final of the impact, and in table 7.2.2 results obtained until the moment of double side failure.

Table 7.2.1 – structure TYPE2 results centralizing - total

Structure	Energie internă totală	Diferenţă Energie internă totală	Deplasare maximă	Diferenţă Deplasare maximă	Masă	Diferenţă masă	Energie internă totală/masă structure
	[MJ]	%	[m]	%	[t]	%	[MJ / t]
Structure conv.	5.318	-	-2.100	-	11,88	-	0,448
K-TYPE1	5.148	-3,2%	-1.705	-18,8%	12,84	8,1%	0,401
SANDWICH-TYPE2	4.859	-8,6%	-1.623	-22,7%	13,50	13,6%	0,360

Table 7.2.2 – structure TYPE2 results centralizing - rupere

Structure	Moment rupere dublu bordaj	Energie internă rupere	Diferenţă Energie internă rupere	Deplasare până la rupere	Diferenţă Deplasare până la rupere	Energie internă rupere/masă structure
	[s]	[MJ]	%	[m]	%	[MJ / t]
Structure conv.	0.440	3.830	-	-1.410	-	0,322
K-TYPE1	0.462	4.330	13,1%	-1.444	2,4%	0,337
SANDWICH-TYPE2	0.480	4.321	12,8%	-1.468	4,1%	0,320

7.3 Unconventional structure of double side „SANDWICH” – TYPE3

7.3.1 Structure description TYPE3

Structure TYPE3 consists in adding to conventional structure of the following elements (figure 7.3.1):

- one layer of polystyrene 140 mm thick on the inner side shell,
- one layer of steel 4 mm thick applied over the polystyrene of inner side, such that it results an sandwich shell for the inner side made from steel-polystyrene-steel.

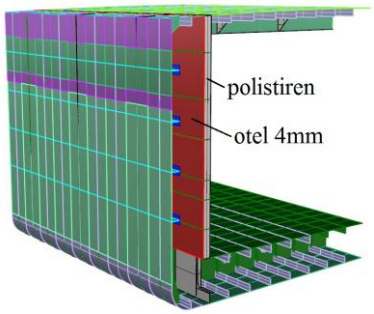

Fig.7.3.1 – Model 3D – structure TYPE3

7.3.3 Structure analyse TYPE3 in plastic deformation with dynamic load

In table 7.3.1 are presented comparative between the conventional structure, structure TYPE1, structure TYPE2 and structure TYPE3, results obtained until the final of the impact, and in table 7.3.2 results obtained until the moment of double side failure.

Table 7.3.1 – structure TYPE3 results centralizing - total

Structure	Energie internă totală	Diferenţă Energie internă totală	Deplasare maximă	Diferenţă Deplasare maximă	Masă	Diferentă masă	Energie internă totală/masă structure
	[MJ]	%	[m]	%	[t]	%	[MJ / t]
Structure conv.	5.318	-	-2.100	-	11,88	-	0,448
K-TYPE1	5.148	-3,2%	-1.705	-18,8%	12,84	8,1%	0,401
SANDWICH-TYPE2	4.859	-8,6%	-1.623	-22,7%	13,50	13,6%	0,360
SANDWICH-TYPE3	5.139	-3,4%	-1.781	-15,2%	12,73	7,15%	0,404

Table 7.3.2 – structure TYPE3 results centralizing - rupere

Structure	Moment rupere dublu bordaj	Energie internă rupere	Diferenţă Energie internă rupere	Deplasare până la rupere	Diferenţă Deplasare până la rupere	Energie internă rupere/masă structure
	[s]	[MJ]	%	[m]	%	[MJ / t]
Structure conv.	0.440	3.830	-	-1.410	-	0,322
K-TYPE1	0.462	4.330	13,1%	-1.444	2,4%	0,337
SANDWICH-TYPE2	0.480	4.321	12,8%	-1.468	4,1%	0,320
SANDWICH- TYPE3	0.477	4.265	11,4%	-1.538	9,1%	0,335

7.4 Unconventional structure of double side „SANDWICH” – TYPE4

7.4.1 Structure description TYPE4

Structure TYPE4 consists in adding to conventional structure of the following elements (figure 7.4.1):

- one layer of polystyrene 160 mm thick on the outer side shell,
- one layer of Epoxy S-Glass UD 10 mm thick applied over the polystyrene of outer side, such that it results an sandwich shell for the outes side made from steel-polystyrene-GRP
- one layer of polystyrene 140 mm thick on the inner side shell,
- one layer of Epoxy S-Glass UD 10 mm thick applied over the polystyrene of inner side, such that it results an sandwich shell for the inner side made from steel-polystyrene-GRP

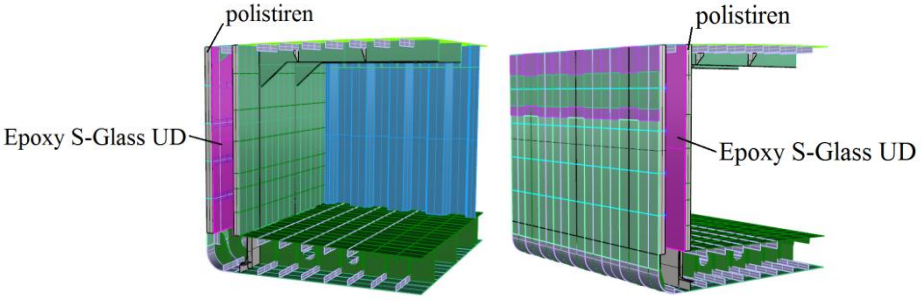

Fig.7.4.1 – Model 3D – structure TYPE4

7.4.3 Structure analyse TYPE4 in plastic deformation with dynamic load

In table 7.4.1 are presented comparative between the conventional structure, structure TYPE1, structure TYPE2, structure TYPE3 and structure TYPE4 results obtained until the final of the impact, and in table 7.4.2 results obtained until the moment of double side failure.

Table 7.4.1 – structure TYPE4 results centralizing - total

Structure	Energie internă totală	Diferenţa Energie internă totală	Deplasare maximă	Diferenţa Deplasare maximă	Masă	Diferenţa masă	Energie internă totală/masă structure
	[MJ]	%	[m]	%	[t]	%	[MJ / t]
Structure conv.	5.318	-	-2.100	-	11,88	-	0,448
K-TYPE1	5.148	-3,2%	-1.705	-18,8%	12,84	8,1%	0,401
SANDWICH-TYPE2	4.859	-8,6%	-1.623	-22,7%	13,50	13,6%	0,360
SANDWICH-TYPE3	5.139	-3,4%	-1.781	-15,2%	12,73	7,15%	0,404
SANDWICH-TYPE4	4.563	-14,2%	-1.630	-22,4%	13,10	10,3%	0,348

Table 7.4.2 – structure TYPE4 results centralizing - rupere

Structure	Moment rupere dublu bordaj	Energie internă rupere	Diferenţa Energie internă rupere	Deplasare până la rupere	Diferenţa Deplasare până la rupere	Energie internă rupere/masă structure
	[s]	[MJ]	%	[m]	%	[MJ / t]
Structure conv.	0.440	3.830	-	-1.410	-	0,322
K-TYPE1	0.462	4.330	13,1%	-1.444	2,4%	0,337
SANDWICH-TYPE2	0.480	4.321	12,8%	-1.468	4,1%	0,320
SANDWICH-TYPE3	0.477	4.265	11,4%	-1.538	9,1%	0,335
SANDWICH-TYPE4	0.480	4.012	4,8%	-1.476	4,7%	0,306

7.5 Unconventional structure of double side „ICE” – TYPE5

7.5.1 Structure description TYPE5

Structure TYPE5 consists in adding of the following elements (figure 7.5.1):

- flange 100 x 8 mm at every simple frame
- intermediate frames „T” profile 160 x 5,6/100 x 8 mm
- bracket between deck and double side, inside double side 480x260x6,5 mm
- bracket between deck and double side, inside cargo tank 800x425x6,5 mm with flange 40x6,5 mm and FB in continuation of the bracket for stiffening deck shell 1000x140x6,5mm
- bilge bracket 6,4 mm thick with flange 100x6,4 mm and FB in continuation of the bracket for stiffening of bottom shell 1325x120x6,4mm
- FB for stiffening of double bottom 1000x160x6,5mm

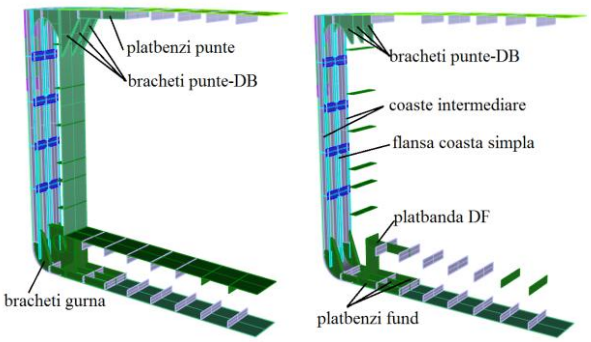

Fig.7.5.1 – Model 3D – structure TYPE5

7.5.3 Structure analyse TYPE5 in plastic deformation with dynamic load

In table 7.5.1 are presented comparative between the conventional structure, structure TYPE1, structure TYPE2, structure TYPE3, structure TYPE4 and structure TYPE5 results obtained until the final of the impact, and in table 7.5.2 results obtained until the moment of double side failure.

Table 7.5.1 – structure TYPE5 results centralizing - total

Structure	Energie internă totală	Diferenţă Energie internă totală	Deplasare maximă	Diferenţă Deplasare maximă	Masă	Diferenţă masă	Energie internă totală/masă structure
	[MJ]	%	[m]	%	[t]	%	[MJ / t]
Structure conv.	5.318	-	-2.100	-	11,88	-	0,448
K-TYPE1	5.148	-3,2%	-1.705	-18,8%	12,84	8,1%	0,401
SANDWICH-TYPE2	4.859	-8,6%	-1.623	-22,7%	13,50	13,6%	0,360
SANDWICH-TYPE3	5.139	-3,4%	-1.781	-15,2%	12,73	7,15%	0,404
SANDWICH-TYPE4	4.563	-14,2%	-1.630	-22,4%	13,10	10,3%	0,348
ICE-TYPE5	4.964	-8,5%	-1.819	-13,4%	13,71	15,4%	0,362

Table 7.5.2 – structure TYPE5 results centralizing - rupere

Structure	Moment rupere dublu bordaj	Energie internă rupere	Diferenţă Energie internă rupere	Deplasare până la rupere	Diferenţă Deplasare până la rupere	Energie internă rupere/masă structure
	[s]	[MJ]	%	[m]	%	[MJ / t]
Structure conv.	0.440	3.830	-	-1.410	-	0,322
K-TYPE1	0.462	4.330	13,1%	-1.444	2,4%	0,337
SANDWICH-TYPE2	0.480	4.321	12,8%	-1.468	4,1%	0,320
SANDWICH-TYPE3	0.477	4.265	11,4%	-1.538	9,1%	0,335
SANDWICH-TYPE4	0.480	4.012	4,8%	-1.476	4,7%	0,306
ICE-TYPE5	0.340	3.061	-20,1%	-1.188	-15,7%	0,223

7.6 Unconventional structure of double side „DUCTIL” – TYPE6

7.6.1 Structure description TYPE6

Structure TYPE6 consists in replacing the inner side shell winth a more ductil steel, for example stainless steel 304L, 316L, 317 LN having bracking elongation 45% (figure 7.6.1).

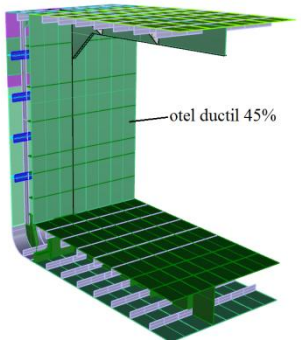

Fig.7.6.1 – Model 3D – structure TYPE6

7.6.3 Structure analyse TYPE6 in plastic deformation with dynamic load

In table 7.6.1 are presented comparative between the conventional structure, structure

TYPE1, structure TYPE2, structure TYPE3, structure TYPE4, structure TYPE5 and structure TYPE6 results obtained until the final of the impact, and in table 7.6.2 results obtained until the moment of double side failure.

Table 7.6.1 – structure TYPE6 results centralizing - total

Structure	Energie internă totală	Diferenţă Energie internă totală	Deplasare maximă	Diferenţă Deplasare maximă	Masă	Diferenţă masă	Energie internă totală/masă structure
	[MJ]	%	[m]	%	[t]	%	[MJ / t]
Structure conv.	5.318	-	-2.100	-	11,88	-	0,448
K-TYPE1	5.148	-3,2%	-1.705	-18,8%	12,84	8,1%	0,401
SANDWICH-TYPE2	4.859	-8,6%	-1.623	-22,7%	13,50	13,6%	0,360
SANDWICH-TYPE3	5.139	-3,4%	-1.781	-15,2%	12,73	7,15%	0,404
SANDWICH-TYPE4	4.563	-14,2%	-1.630	-22,4%	13,10	10,3%	0,348
ICE-TYPE5	4.964	-8,5%	-1.819	-13,4%	13,71	15,4%	0,362
DUCTIL-TYPE6	5.806	9,2%	-1.872	-10,8%	11,88	0,0%	0,489

Table 7.6.2 – structure TYPE6 results centralizing - rupere

Structure	Moment rupere dublu bordaj	Energie internă rupere	Diferenţă Energie internă rupere	Deplasare până la rupere	Diferenţă Deplasare până la rupere	Energie internă rupere/masă structure
	[s]	[MJ]	%	[m]	%	[MJ / t]
Structure conv.	0.440	3.830	-	-1.410	-	0,322
K-TYPE1	0.462	4.330	13,1%	-1.444	2,4%	0,337
SANDWICH-TYPE2	0.480	4.321	12,8%	-1.468	4,1%	0,320
SANDWICH-TYPE3	0.477	4.265	11,4%	-1.538	9,1%	0,335
SANDWICH-TYPE4	0.480	4.012	4,8%	-1.476	4,7%	0,306
ICE-TYPE5	0.340	3.061	-20,1%	-1.188	-15,7%	0,223
DUCTIL-TYPE6	-	5.806	51,6%	-	-	0.489

7.7 Unconventional structure of double side „LIGHT" – TYPE7

7.7.1 Structure description TYPE7

Structure TYPE7 consists in reducing the weight of the conventional structure elements (figure 7.7.1):

- Deck web frames – cutouts 150 x 300 mm
- floor – cutouts ϕ 300 mm
- lateral floor – cutouts 380 x 500 mm

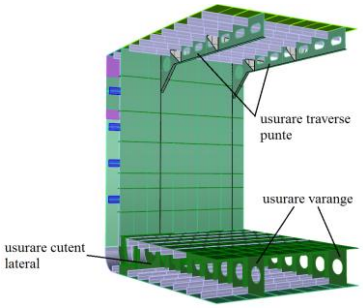

Fig.7.7.1 – Model 3D – structure TYPE7

7.7.3 Structure analyse TYPE7 in plastic deformation with dynamic load

In table 7.7.1 are presented comparative between the conventional structure, structure TYPE1, structure TYPE2, structure TYPE3, structure TYPE4, structure TYPE5, structure TYPE6 and structure TYPE7 results obtained until the final of the impact, and in table 7.7.2 results obtained until the moment of double side failure.

Table 7.7.1 – structure TYPE7 results centralizing - total

Structure	Energie	Diferenta	Deplasare	Diferenţă	Masă	Diferenţă	Energie
	[MJ]	%	[m]	%	[t]	%	[MJ / t]
Structure conv.	5.318	-	-2.100	-	11,88	-	0,448
K-TYPE1	5.148	-3,2%	-1.705	-18,8%	12,84	8,1%	0,401
SANDWICH-	4.859	-8,6%	-1.623	-22,7%	13,50	13,6%	0,360
SANDWICH-	5.139	-3,4%	-1.781	-15,2%	12,73	7,15%	0,404
SANDWICH-	4.563	-14,2%	-1.630	-22,4%	13,10	10,3%	0,348
ICE-TYPE5	4.964	-8,5%	-1.819	-13,4%	13,71	15,4%	0,362
DUCTIL-TYPE6	5.806	9,2%	-1.872	-10,8%	11,88	0,0%	0,489
LIGHT-TYPE7	5.369	1,0%	-2.080	-1,0%	11,50	-3,2%	0,467

Table 7.7.2 – structure TYPE7 results centralizing - rupere

Structure	Moment	Energie	Diferenţă	Deplasare	Diferenţă	Energie
	[s]	[MJ]	%	[m]	%	[MJ / t]
Structure conv.	0.440	3.830	-	-1.410	-	0,322
K-TYPE1	0.462	4.330	13,1%	-1.444	2,4%	0,337
SANDWICH-	0.480	4.321	12,8%	-1.468	4,1%	0,320
SANDWICH-	0.477	4.265	11,4%	-1.538	9,1%	0,335
SANDWICH-	0.480	4.012	4,8%	-1.476	4,7%	0,306
ICE-TYPE5	0.340	3.061	-20,1%	-1.188	-15,7%	0,223
DUCTIL-TYPE6	-	5.806	51,6%	-	-	0.489
LIGHT-TYPE7	0.452	3.663	-4,4%	-1.535	8.9%	0.319

7.8 Unconventional structure of double side „ARC” – TYPE8

7.8.1 Structure description TYPE8

Structure TYPE8 consists in adding to conventional structure of the following elements (figure 7.8.1):

- transversal stiffeners 6,5 mm thick on the inner side arc shape with 1500 mm radius, connected to deck and double bottom
- reducing the weight of deck transvers webs, floors and lateral floor identical chapter 7.7.

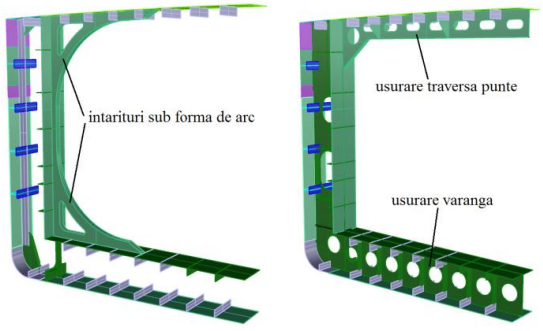

Fig.7.8.1 – Model 3D – structure TYPE8

7.8.3 Structure analyse TYPE8 in plastic deformation with dynamic load

In table 7.8.1 are presented comparative between the conventional structure, structure TYPE1, structure TYPE2, structure TYPE3, structure TYPE4, structure TYPE5, structure TYPE6, structure TYPE7 and structure TYPE8 results obtained until the final of the impact, and

in table 7.8.2 results obtained until the moment of double side failure.

Table 7.8.1 – structure TYPE8 results centralizing - total

Structure	Energie	Diferenţă	Deplasare	Diferenţă	Masă	Diferenţă	Energie
	[MJ]	%	[m]	%	[t]	%	[MJ / t]
Structure conv.	5.318	-	-2.100	-	11,88	-	0,448
K-TYPE1	5.148	-3,2%	-1.705	-18,8%	12,84	8,1%	0,401
SANDWICH-	4.859	-8,6%	-1.623	-22,7%	13,50	13,6%	0,360
SANDWICH-	5.139	-3,4%	-1.781	-15,2%	12,73	7,15%	0,404
SANDWICH-	4.563	-14,2%	-1.630	-22,4%	13,10	10,3%	0,348
ICE-TYPE5	4.964	-8,5%	-1.819	-13,4%	13,71	15,4%	0,362
DUCTIL-TYPE6	5.806	9,2%	-1.872	-10,8%	11,88	0,0%	0,489
LIGHT-TYPE7	5.369	1,0%	-2.080	-1,0%	11,50	-3,2%	0,467
ARC-TYPE8	5.633	5,9%	-1.820	-13,3%	12,62	6,2%	0,446

Table 7.8.2 – structure TYPE8 results centralizing - rupere

Structure	Moment	Energie	Diferenţă	Deplasare	Diferenţă	Energie
	[s]	[MJ]	%	[m]	%	[MJ / t]
Structure conv.	0.440	3.830	-	-1.410	-	0,322
K-TYPE1	0.462	4.330	13,1%	-1.444	2,4%	0,337
SANDWICH-	0.480	4.321	12,8%	-1.468	4,1%	0,320
SANDWICH-	0.477	4.265	11,4%	-1.538	9,1%	0,335
SANDWICH-	0.480	4.012	4,8%	-1.476	4,7%	0,306
ICE-TYPE5	0.340	3.061	-20,1%	-1.188	-15,7%	0,223
DUCTIL-TYPE6	-	5.806	51,6%	-	-	0.489
LIGHT-TYPE7	0.452	3.663	-4,4%	-1.535	8.9%	0.319
ARC-TYPE8	0.690	5.614	46,6%	-1.813	28.6%	0.445

7.9 CONCLUSIONS

Analyzing the results obtained for unconventional structure solutions investigated, it cand be drawn the following conclusins:

a) One method for increasing the deformation energy is adding of some structure elements which to participate to the impact (TYPE1, TYPE2, TYPE3, TYPE4, TYPE5, TYPE8), this approach leading to increasing the structure weight. To be noted that the increasing rate of the internal energy until the moment of tank shell rupture do not depends only on the mass of the added elements, but rather on the structural arrangement which leads to involvement of existing and additional structure elements during the impact.

b) another method for increasing the internal energy until the tank shall failure is using of more ductile materials (TYPE6), which to delay the rupture of the double side and to permit the structure to absorb more deformation energy until that moment. This solution practical keeps or even reduces the mass of the structure in comparison with conventional structure, for the same level of deformation energy until the tank rupture.

c) reducing the weight of the elements with a low participation to the deformation energy (TYPE7) didn’t modified the total energy of deformation and nor the maximum displacement of the bow model.This principle may be used at designing of future structures in order to reduce the weight.

CHAPTER 8
PROPOSALS FOR EXISTING STRUCTURE MODERNIZATION

In the following are proposed several solutions for modernization of existing double hull structures, specifying each one the advantages and disatvantages:

A) Proposal „Ductil" – TYPE6

Modernization suppose:

- replacing the side shell with an more ductil steel, having failure elongation 45%.

Advantages:

- maximum increasing of deformation energy – if the mai goal is internal energy increasing than this solution is the best (51,6% compared with conventional structure)
- structure weight – practical is keep the same weight of conventional structure, which leads to maixum ratio 0,489 MJ/t

Disadvantages:

- implementation of this solution to an existing structure suppose removal of double side shell, keeping the existing stiffeners and assembly of the new shell made from „ductil" steel, which involves an expensive workmanship
- „ductil" steel must be supplied and the cost must be investigated comparative to usual ship steel

B) Proposal „ARC" – TYPE8

Modernization suppose:

- adding the transverse stiffeners „arc" type at the interior of the side, having 6,5 mm thickness
- reducing the weight of the deck web frames, floors and lateral floor of double bottom.

Advantages:

- big deformation energy increasing (46,6% compared with conventional structure)
- structure weight – is realized the smallest increase of weight, with 6,2% to conventional structure, obtaining thus second position as energy ratio 0,445 MJ/t
- simple technology – practical „arc" type elements are done from usual steel and with usual technology from shipyards

Disadvantages:

- in some situations, like more viscous substances: oil, asphalt etc., added „arc" elements in the interior of the cargo tanks can creat functional problems (cargo heating system complications, accumulation of transported substances around the structure elements, making worse the washing process of cargo tanks)
- can not be applied at ships for bulk cargo or container transporting ships

C) Proposal „K" – TYPE1

Modernization suppose:

- adding of some deformable girder type elements between the outer side ant deck and between the outer shell and double bottom
- adding of some brackets between the double side and deck and between the double side and double bottom.

Advantages:

- good deformation energy increasing (13,1% to conventional structure)
- bow model penetration – it reduces significantly the maximum penetration, with 18,8%
- simple technology – additional structure elements are done from „I" profiles existing/welded, being done from usual steel and assembled by welding
- can be applied to any type of ship, additional structural elements are provided only

inside the double hull space

Disadvantages:

- small energy ratio 0,337 MJ/t

B) Proposal „SANDWICH" – TYPE3

Modernization suppose:

- transformation of the outer and inner side shell in a steel-polystyrene-steel sandwich, by adding of an polystyrene layer and then of an steel layer.

Advantages:

- good deformation energy increase (11,4% to conventional structure)
- structure weight – is obtained a small increase of weight, with 7,15% to conventional structure
- can be applied to any type of ship, additional structural elements are provided only at the interior of the double hull

Disadvantages:

- small energy ratio 0,335 MJ/t
- more expensive fabrication technology
- ballast tank capacity reducing

Conclusions: Each above proposals presents advantages and disadvantages, depending on the importance according to different objectives considered. Thus choosing of one solution or even a combination of solutions will be clearly imposed by the principal objective/objectives followed in the specific case of an double hull structure.

CHAPTER 9
PROPOSAL OF A NEW UNCONVENTIONAL STRUCTURE TYPE-X

Taking in to account the results of chapter 7 and 8 analysis, and also establishing two new objectives structure weight reduction and double side width reduction, was proposed a new unconventional structure, named TYPE-X.

A coupled approach has been attempted for elastic and plastic behavior, such that to result a more efficient structure from weight point of view and from conjugated response to global, local and impact loads point of view.

Design theme

It will be designed a double hull structure for inland tankes ship described in chapter 6.1, which to comply with the following requirements:

- using of usual materials and technology for ship building
- structural strength global and local in elastic behavior according the classification societies rules (BV Rules, 2016)
- ensuring the impact protection of cargo tanks according ADN, 2017
- ensuring the access in adiacent spaces of cargo tanks according ADN, 2017.

Objectives

Supplementary to the above requirements, was proposed fulfillment of the following objectives for unconventional structure TYPE-X:

- reducing the structure weight which lead to the following economical benefits:
    - reducing the construction cost of the ship
    - reducing the draft or increasing the deadweight
- reducing the width of double side or the height of double bottom leading thus to flexibility in structural arrangement
- to ensure at least the same impact strength like the conventional structure.

Strategy

In present the ship structure design approach in general only the problem of elastic behavior strength, so the arrangement and scantling of the structure are thought for an optimum response at global an local loads under elastic behavior limits.

The behavior of the structure at collision is investigated only in some situation according specific requirements, for the exmaple NMA 123/1994 sau ADN 2017.

Is obvious that the separation of this two approaches most of the time do not leads to a structure with an efficient response for both behaviors.

Practical the unconventional structure TYPE-X was designed as follows:

a) were keeped the main longitudinal strength elements: structure of deck, bottom and double bottom identical with conventional ship, just for highlight only the benefits of the unconventional structure of double side proposed

b) redesigning the side and double side structure, which to respond conjugated at local loads (outer shell sea pressure, tank cargo pressure) and at loadings from side collision with another ship. For that purpose were considered the solutions investigated in chapter 7.

c) verifying of the structure in elastic behavior by finit element analyse, according chapter 6.2

d) verifying the structure at collision, according chapter 6.4.

Phases b)...d) were resumed in an iterative process, modifying the structure elements until was found the most efficient solution from weight point of view and of conjugated response to all the loadings considered.

9.1 Unconventional structure TYPE-X analyse in elastic behavior

Unconventional structure TYPE-X consists in implementation of the following solution:

- reducing the weight of deck web frames, floors and lateral floor of double bottom
- reducing the width of double side with 60mm
- using of more ductil steel at double side shell, with breaking elongation 30%
- removal of longitudinal stiffeners and adoption of an transverse stiffners system for double side made from „ARC” type elements and HP 120x7 profile frames
- removal the outer side stringhers.

In figures 9.1 - 9.5 are presented an overview of the structure and also every frame type modified.

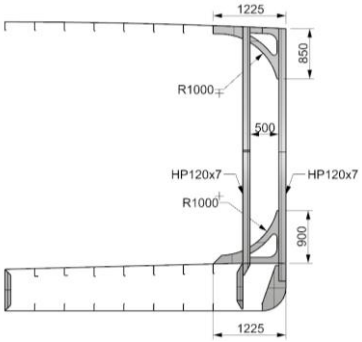

Fig.9.1–Simple frame-structure TYPE-X

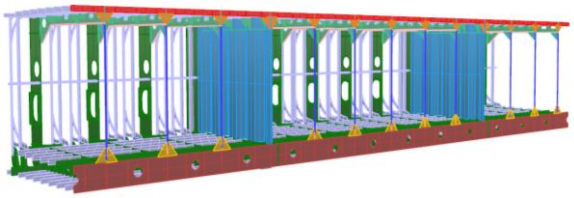

Fig.9.3–Model 3D–structure TYPE-X

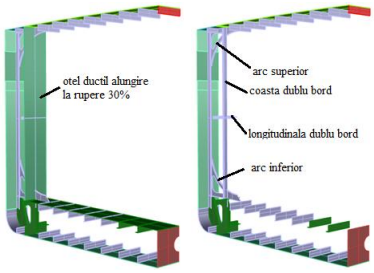

Fig.9.4–Model 3D–simple frame

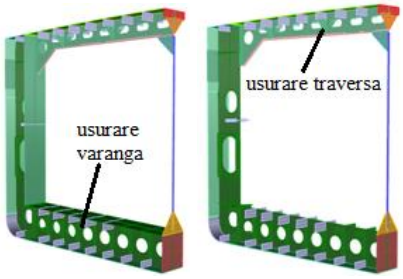

Fig.9.5–Model 3D–web frame

In figure 9.6 is presented unconventional structure TYPE-X elements meshing.

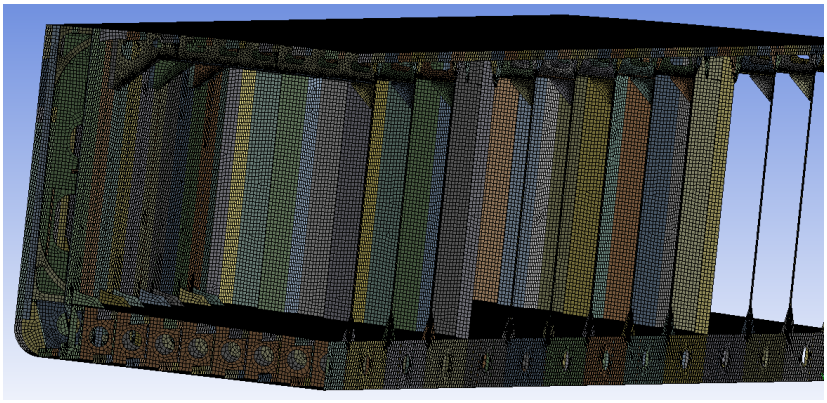

Fig.9.6 – Structure TYPE-X meshing

Calculation results

In table 9.1 below was considered the maximum value of σ_{FEM} stress resulted from the four loading cases considered (A1, A2, B1 and B2) for every structure elements.

Table 9.1 – stress level in unconventional structure of double side TYPE-X

Nr.	**Denumire element**	**z**	**Z**	**σ_{HGL}**	**σ_{FEM}**	**σtotal**
		[m]	[cm3]	[MPa]	[MPa]	[MPa]
1	Tablă lacrimară	4.79	621937	57	14	71
2	Centură	4.758	629531	56	20	76
3	Tablă bordaj 1	4.2	799806	44	37	81
4	Tablă bordaj 2	3.57	1151431	31	47	78
5	Tablă bordaj 3	3.3	1418745	25	85	110
6	Tablă gurnă	0	772110	46	43	89
7	Tablă dublu bord	4.79	621937	57	118	175
8	Diafragmă bordaj etanşă				43	43
9	Diafragmă bordaj				172	172
10	Coastă bordaj HP120x7				113	113
11	Brachet gurnă				16	16
12	Coastă dublu bordaj HP120x7				143	143
13	Elemente de TYPE “arc”				171	171
14	Longitudinală dublu bordaj T 120x7/60x7	2.70	2930728	12	155	167
15	Curent lateral Y3925	0	772110	46	54	100
16	Bracheţi diafragmă bordaj etanşă				65	65
17	Nervuri diafragmă bordaj 100x8				57	57
18	Longitudinale punte HP140x7	4.79	621937	57	10	67
19	Longitudinale fund HP 120x7	0	772110	46	16	62

Conclusion: The table 9.1 above shows that the values of stress are under admissible limit σ_{VM} = 219,3 MPa.

In figures 9.7...9.10 are presented the stress distribution and structure deformation under local loads.

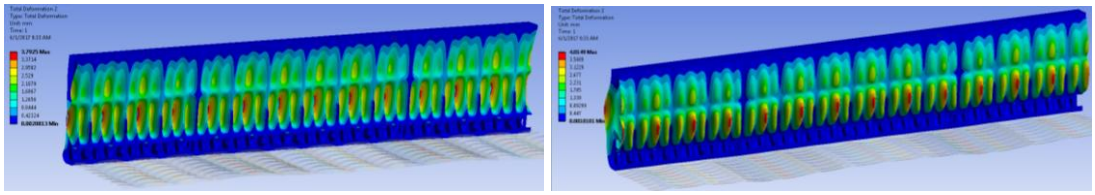

Fig.9.9 – Double side TYPE-X deformation – loading case A2 and B1

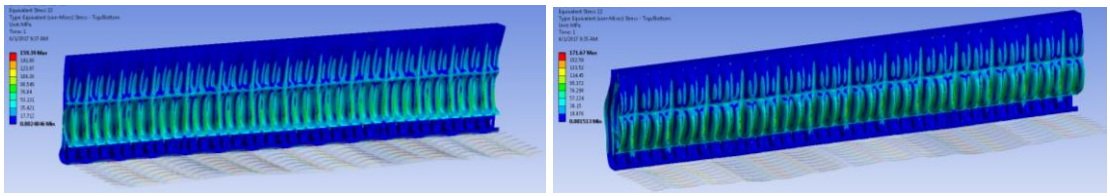

Fig.9.10 – Stress distribution in double side TYPE-X - loading case A2 and B1

9.2 Structure analyse neconventională TYPE-X in plastic deformation with dynamic load

For this analyse was used mode ductil steel, having yield stress R_Y = 236,2 MPa, tangent modulus 1105 MPa and breaking elongation 30%.

9.2.2 Double side failure

Analysing the equivalent stress distribution, at different intermediate moments, the following inner side rupture causes were identified:

- rupture of elements in a horizontal plane corresponding to contact between bow model deck and double side, at moment t = 0,69 s
- rupture of elements on a vertical direction because the contact between the bow model stem and double side.

In figure 9.14 is presented the failure of tank shell in a view from outside of the tank to the double side.

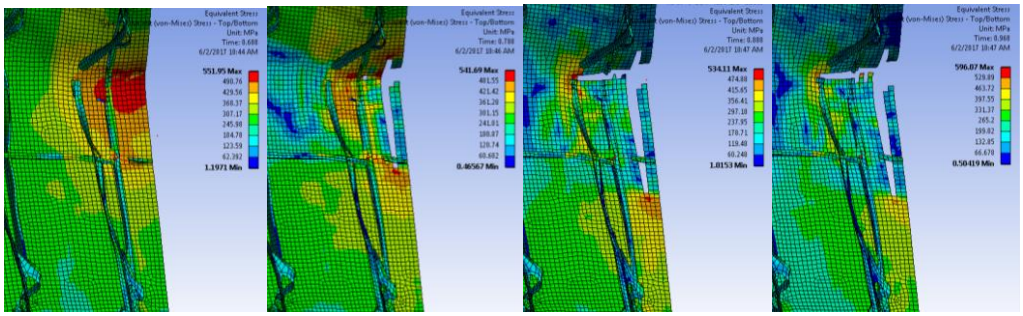

Fig.9.14 – Contact area between bow model and double side shell – structure TYPE-X

9.2.5 Energy and displacements

In figure 9.17 is presented the kinetic energy diagram [MJ] of bow model depending on time.

In figure 9.18 is presented the internal energy diagram [MJ] depending on time.

In figure 9.19 is presented the bow model displacement diagram [m] on Oy direction of structure model depending on time.

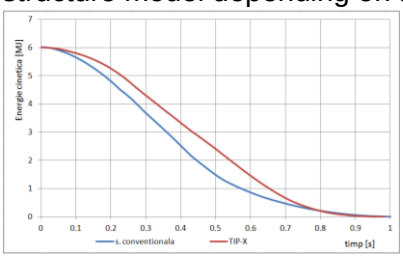

Fig.9.17–Kinetic energy

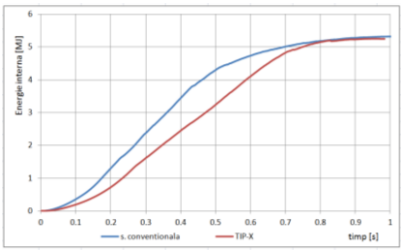

Fig.9.18–Internal energy

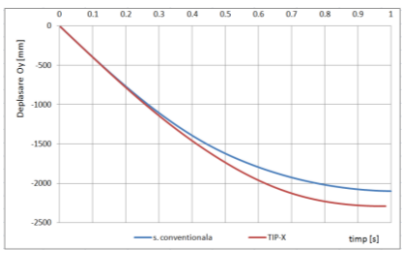

Fig.9.19–Bow displacement

Conclusions In table 9.2 are presented comparative between the conventional structure and structure TYPE-X results obtained until the final of the impact, and in table 9.3 results obtained until the moment of double side failure.

Table 9.2 – centralizator rezultate structure TYPE-X - total

Structure	Energie internă totală	Diferenţă Energie internă totală	Deplasare maximă	Diferenţă Deplasare maximă	Masă	Diferenţă masă	Energie internă totală/masă structure
	[MJ]	%	[m]	%	[t]	%	[MJ / t]
Structure conv.	5.318	-	-2.100	-	11,88	-	0,448
TYPE-X	5.255	-1,2%	-2.288	8,9%	10,74	-9,6%	0,489

Table 9.3 – centralizator rezultate structure TYPE-X - rupere

Structure	Moment rupere dublu bordaj	Energie internă rupere	Diferenţă Energie internă rupere	Deplasare până la rupere	Diferenţă Deplasare până la rupere	Energie internă rupere/masă structure
	[s]	[MJ]	%	[m]	%	[MJ / t]
Structure conv.	0.440	3.830	-	-1.410	-	0,322
TYPE-X	0.690	4.772	24,6%	-2.112	49,7%	0,444

Conclusions: Unconventional proposed new structure TYPE-X comply with the requirements regarding the global and local structural strength for elastic behavior and ADN requirements for access in adiacent spaces to cargo tanks.

Structure TYPE-X satisfied the proposed objectives thus:

- reducing the structure weight with 10%
- raducing the double side width with 7,5%
- impact deformation energy higher with 25% then conventional structure.

In order to obtain the impact deformation energy was used an more ductil steel, with breacking elongation of minimum 30%, appearing the necessity to create a new steel, with higher ductility, in case this is not already on the market with a reasonable price.

CHAPTER 10
FINAL CONCLUSIONS

Using of double hull structure is based on two general justifications:

- complying with some general functions: ensuring the spaces for ballast and reserves tanks and hull subdivision for damage stability
- complying with some specific functions to every type of ship: cargo tank protection, ensuring a precise geometry at tank interior for technical ships etc.

In general, from strength point of view, double hull structures were designed to respond the elastic behavior requirements.

In the last period developed the structure analyse in plastic deformation behavior, in this regard appeared a series of rules which indicates the analyse mode and the requirements for structure behavior at grounding or side collision.

IMO, IACS and other authorities in ship construction field have adopted rules regarding the compulsory of double hull structures and also the constructive measures.

Such rules that impose the double hull structures, are:

- MARPOL – double bottom and double side for pollution prevention
- SOLAS – double bottom for damage stability
- MSC.235(52) – double side for pollution prevention
- IBG, IGC, ADN and NMA 123/1994– double bottom and double side for pollution prevention.

Constructive measures imposed to double hull structures consists in general in a series of tules for scantling and arrangement, and only in certain situations being necessary direct analyse.

The study of ship structure behavior at collision is done by direct analyse with finit element analyse, with help of which can be demonstrated the efficiency of some structure in case of the impact scenarios imposed by specific rules (ADN, NMA 123/1994).

Using the finit element method at ship structures analyse is regulated by ship classification societies Rules and by other authorities, the concrete aspects referring to being:

- net thickness
- model extending
- structure meshing in finit elements
- boundary conditions application
- loading application
- stress calculations
- material idealization
- failure criteria

To determine the level of approximation of calculation methodology proposed for the analyse of structure behavior in plastic deformations were done a series of experimental tests, consisting in elasto-plastic deformation of three structure models with help of a spheric bulb :

- experiment 1 – simple steel panel
- experiment 2 – stiffened steel panel
- experiment 3 – steel-XPS polystyrene-steel sandwich panel.

Durring the experiments were measured:

- contact force between spherical bulb and steel panel of the model
- vertical displacement of the model (force application direction).

The numerical simulation of the experimental test were done to investigate the influence of meshing, boundary conditions and material idealization to the results.

After the comparative analyse between the experiments and afferent numerical simulations resulted the following differences expressed in procents, presented in table 10.1 below:

Table 10.1 – comparative centralizing experiments-simulations

		Diferențe [%]
Nr.	**Experiment**	**Deformată plastică**
1	**Experiment 1**	4.00
2	**Experiment 2**	2.70
3	**Experiment 3**	2.86

It can be observed that maximum difference for plastic deformation between the experiments and numerical simulations is of maximum 4%.

Maximum error level possible during the experiments, because the measuring tools and the test stand, totals 2%.

Considering the worst case scenario, when all errors sums up, will result a total difference, for plastic deformations, between the experiment and numerical simulation of 2% + 4% = 6%.

Considering the safety margin used in ship structure field, in general between 5% and 10 %, it can be concluded that the error level between the experiments done and numerical simulations based on the analyse method considered is falling in acceptet error marge.

The analyse method proposed for investigation of double hull structures and calibrated based on the experiments was used first to analyse the behavior of conventional structure at side collision and then at analyse of different unconventional structure solutions.

The reference structure used at comparative analyse is a inland tanker ship structure for dangerous goods transportation, designed according AND requirements.

Analyzing the results obtained after the numerical simulation of side collision, according ADN, for the conventional structure the following were concluded:

- to be avoided using stiffeners on the oute side which can become stress concentrators at the contact with the inner side shell, thus leading to failure of the last one (see 6.4.5.2),
- to be avoided using at inner side of elements with great stiffness differences in OY direction, the deformation direction imposed by bow model (see 6.4.5.2),
- considering the deformation energy it can be appreciated the level of participation for every structure element durring the impact and it can be redesigned the structure such that results a weight reduction simultaneous with a similar energy absorbtion capacity (see 6.4.5.3),
- analyzing the local behavior of structure elements it can be identified different solution for increasing the level of total energy absorbtion of structure during the collision (see 6.4.5.4).

Analysing the deformation mode of conventional structure at impact, the areas where appear the stress concentrators, the failure mode of tank shell were identified the following solutions to be investigated:

- using some structure elements which to transmit the energy from highly loaded zones to less loaded zones – **structure „K”** (TYPE1)
- using of some elements which to dissipate the stress concentrators that leads to material failure – **structure „SANDWICH”** (TYPE2, TYPE3, TYPE4)
- reinforcing the outer side – **structure „ICE”** (TYPE5)
- using a more ductil material at inner side shell – **structure „DUCTIL”** (TYPE6)
- reducing the weight of structure elements with low participation to deformation energy – **structure „LIGHT”** (TYPE7)
- reinforcing the inner side – **structure „ARC”** (TYPE8)

After the investigation of the above solutions for unconventional structures the following conclusions can be drawn:

- One method for increasing the deformation energy is adding of some structure elements which to participate to the impact (TYPE1, TYPE2, TYPE3, TYPE4, TYPE5, TYPE8), this approach leading to increasing the structure weight. To be noted that the increasing rate of the internal energy until the moment of tank shell rupture do not depends only on

the mass of the added elements, but rather on the structural arrangement which leads to involvement of existing and additional structure elements during the impact.

- another method for increasing the internal energy until the tank shall failure is using of more ductile materials (TYPE6), which to delay the rupture of the double side and to permit the structure to absorb more deformation energy until that moment. This solution practical keeps or even reduces the mass of the structure in comparison with conventional structure, for the same level of deformation energy until the tank rupture.
- reducing the weight of the elements with a low participation to the deformation energy (TYPE7) didn't modified the total energy of deformation and nor the maximum displacement of the bow model.This principle may be used at designing of future structures in order to reduce the weight.

Each of the proposed solution presents advantages and disadvantages, such that the choosing of one solution or even a combination of solutions will be dictaded by the main objective/objectives followed in specific case of a double hull structure.

Considering the results obtained previously and the two main objectives: reducing the structure weight and reducing the width of double side, an new unconventional structure was proposed, named TYPE-X .

Following analysis was found that the unconventional proposed new structure TYPE-X comply with the requirements regarding the global and local structural strength for elastic behavior and ADN requirements for access in adiacent spaces to cargo tanks.

Structure TYPE-X satisfied the proposed objectives thus:

- reducing the structure weight with 10%
- raducing the double side width with 7,5%
- impact deformation energy higher with 25% then conventional structure.

In order to obtain the impact deformation energy was used an more ductil steel, with breacking elongation of minimum 30%.

In condițiile in care acest TYPE de oțel nu există deja pe piață sau nu exista la un cost rezonabil, apare deci necesitatea de a dezvolta un oțel nou, care să prezinte ductilitate mai mare and să fie fezabil pentru structurile navale.

Thus from the necessity to respond both to requirements of double hull impact behavior, imposed by ADN, and also to objective of reducing the weight of the structure, a new direction of research and innovation is born in material field for ship constructions.

Synthetic conclusions that may come out from this study are:

a) Double hull structures were introduced in ship building in order to increase the safety level of the ship and to reduce the environment pollution risk in case of grounding or side collision.

b) In general the double hull structures are designed according arrangement and scantling regulations imposed by IMO and IACS Rules, direct analyse being necessary only in some situations.

c) The study of ship structures behavior at impact is done through finit element analyse, calculation conditions and the collision scenarios being imposed by specific rules (ADN, NMA 123/1994).

d) In present ship designing is done in general disjunctive regarding the two aspects: elastic behavior and plastic behavior. The structures are designed most of the times for an optimal response in elastic behavior and only in certain situations when rules are imposing are adopted solutions regarding impact structure behavior.

e) Using the finit element method were investigated different solutions for double hull viable for improving the behavior of structures at impact.

f) A unconventional structure of double hull was designed to respond the requirements of Rules and the additional objectives imposed (reducing the structure weight and reducing the width of the double side), using the finit element analyse for elastic and plastic bahavior.

CHAPTER 11
ORIGINAL CONTRIBUTIONS AND PERSPECTIVES

The main goal of the research activity done in this study was developing of an innovative double hull structure, which to respond both requirements regarding structural strength and safety in exploitation, and to some particular objectives, like reducing the structure weight and/or modification of structure arrangement imposed by Rules.

Original contributions

Accomplishment of the stated purpose is based on a series of original contributions, including:
1) Validation through experiment of calculation methodology used at analyse of structure behavior at plastic deformations. Through realization of experimental tests from chapter 5 it could be established that the approximation level of numerical simulations results compared with the experiment measured vaules are within the accepted margin of error.
2) Setting the parameters for finit element calculation used at unconventional double hull structure analyse. It was investigated the influence to numerical simulations results of different parameters like: material idealization, type an size of finit elements, type of meshing grid (uniform and nonuniform), boundary conditions. Having as reference the experimental results it could be determined the best values of stated parameters, such that to obtain a minimal error level between the experiments and numerical simulations.
3) Systematic investigation of different unconventional structure solutions, based on the following principal directions:

- using some structure elements which to transmit the energy from highly loaded zones to less loaded zones („K”, „ARC”)
- using of some elements which to dissipate the stress concentrators that leads to material failure („SANDWICH”)
- increasing the outer side deformation energy, by doubling the stiffeners („ICE”)
- using a more ductil material at inner side shell („DUCTIL”)
- reducing the weight of structure elements with low participation to deformation energy („LIGHT”).

4) Proposal of modernization solutions for existing double hull structure. Depending on the followed objectives and using the results obtained after the analyse of mentioned solutions, were done the following concrete proposals:

- „DUCTIL” – suited for the following objectives: increasing the deformation energy, keeping the structure weight and keeping the stiffener system unchanged
- „ARC” – suited for: increasing of internal energy and using of usual ship steel
- „K”– suited for: increasing of deformation energy, reducing the bow model penetration and using of usual steel
- „SANDWICH” – suited for: increasing of deformation energy and reducing the bow model penetration.

5) Designing of an innovative double side structure. Having as main objectives: weight reduction, reducing of double side width and maintaining of deformation energy at the level of reference structure, was designed a new double side structure which includes two of the previously investigated solutions „ARC” and „DUCTIL”. An couple approach has been attempted

of elastic and plastic behavior analyse, such that to achieve a more efficient structure from weight point of view and also for the conjugated response to global, local and impact loads. Considerable benefits were obtained:

- structure weight reduction with 10%
- double side width reduction with 7,5%
- impact deformation energy with 25% bigger than conventional structure.

Perspectives

For development of research activity presented in this work, it can be considered the following perspectives:

1) Complete approach of double hull structure in plastic behavior, analyzing also the grounding. If it can be obtained similar results with the TYPE-X structure also for double bottom, then global benefits for innovative structure will be much more consistent.
2) Another direction could be investigation of some solutions based on new materials. Depending on the proposed objectives for an unconventional double hull structure appears the necessity of using improved or even completely new materials. Such an example is the solution „DUCTIL", which proved that can be obtained good results using an material with an improved characteristic, in this case increased ductility.
3) Considering the increased interest for impact analyse and for structure optimization, it can be imagined for the future a new approach: competitive design, such that the scantling and arrangement of the structure to give an optimum response (for example from weight point of view) for global, local and impact loads a the same time.
4) In view of the increasing extent of the impact analyse of ship structure, it would be useful some 1:1 scale experiments, which to permit the adjustment of calculation methods, in woy to obtain a better approximation level.
5) Taking into account the increasing standards of safety and the increased care to the environment, may be predicted in the future the necessity for the large scale anlaysis of the behavior of the ship structures at collision. Thus may be developed and applied a series of rules regarding:

- determination of cargo tank rupture risk in a collision situation
- determination of ship survival capacity after a collision, from structure strength point of view etc.

SELECTIVE BIBLIOGRAPHY

[3] BV Rules, 2016 (NR467) – Bureau Veritas - Rules for the Classifiction of Steel Ships - Edition July 2016;
[8] MARPOL 2006- International Convention for the Prevention of Pollution from Ships – International Maritime Organization 2006;
[9] CSR OT, 2012 – Common Structural rules for Double Hull Oil Tankers – International Association of Classification Societies - July 2012;
[12] CSR BC, 2012 – Common Structural rules for Bulk Carriers – International Association of Classification Societies - July 2012;
[13] ABS, 2015 – American Bureau of Shipping - Rules for Building and Classing Steel Vessels - Edition January 2015;
[14] ADN, 2017 - European Agreement concerning the International Carriage of Dangerous goods by Inland Waterways – United Nations 2016;
[15] http://www.pntl.co.uk/our-fleet/
[16] MOVEIT! - Modernisation of vessels for inland waterway freight traffic http://www.moveit-fp7.eu/
[17] MOVEIT! - Modernisation of vessels for inland waterway freight traffic - Work package WP5 Structures & Weight, Task 5.3 Crashworthiness (TNO, SMILE FEM, University Galati, Ship Design Group, SWEREA Sicomp) – 2014;
[18] Inteligent Engineering UK Limited - http://www.ie-sps.com/sectors/maritime
[19] IE - Inteligent Engineering UK Limited – A member of the IE Group of Companies - January 2016 – Project portofolio;
[23] SOLAS, 2014 – International Convention for the Safety of Life at sea – International Maritime Organization 2014;
[24] MSC.235(82**)** - Guidelines for the design and construction of offshore supply vessels – Maritime Safety Commitee MSC 2006
[25] IBC, 2007 - International Code for the Construction and Equipment of Ships Carrying Dangerous Chemical in Bulk – Maritime Environment Protection Commitee MEPC 2007;
[26] IGC Code, 2016 - International Code for the Construction and Equipment of Ships Carrying Liquefied Gases in Bulk - Maritime Environment Protection Commitee MEPC 2007;
[27] NMA 123/1994 – Norwegian Maritime Autority – Regulations of 10 February 1994 No. 123 for mobile offshore units with production plants and equipment;
[32] Ionel Chirica – Elasticitate – Fundamente. Exemple. Aplicatii – Editura Tehnica, Bucuresti 1997– ISBN 973-31-1129-5;
[35] Chakrabarty J. – Theory of plasticity – Elsevier Butterwoth-Heinemann 2006– ISBN 978-0-7506-6638-2;
[37] Jacob Lubliner – Plasticity theory – Revised edition (PDF) University of California at Berkeley 2006;
[38] E. J. Hearn – Mechanics of materials 1 – Elsevier Butterworth-Heinemann 1997 – ISBN 0-7506-3265-8;
[39] E. J. Hearn – Mechanics of materials 2 – Elsevier Butterworth-Heinemann 1997 – ISBN 0-7506-3266-6;
[40] Philippe Rigo and Enrico Rizzuto – Ship design & Construction, Volume 1 – Chapter 18: *Analysis and Design of Ship Structure* - 2003;
[41] Chen W.F., Han D.J. – Plasticity for Structural Engineers – Springer Verlag New York Inc. 1988 – ISBN 3-540-96711-7;
[43] David Broek – Elementary engineering fracture mechanics – Martinus Nijhoff Publishers 3rd printing 1984 – ISBN 90-247-2580-1;

[45] T.L. Anderson – Fracture mechanics – Fundamentals and Applications – CRC Press LLC 1995 – ISBN 0-8493-4260-0;
[59] ANSYS Release 17 January 2016 – Engineering Data User's Guide;
[60] ANSYS Release 17 January 2016 – ANSYS Explicit Dynamics Analysis Guide;